AAEC/AP PR81
INDC(AUL)-31/G

AAEC/AP PR81
INDC(AUL)-31/G

INIS-XA-N--168

AUSTRALIAN ATOMIC ENERGY COMMISSION

RESEARCH ESTABLISHMENT

LUCAS HEIGHTS

PROGRESS REPORT

APPLIED PHYSICS DIVISION

1 October 1980 to 30 June 1981

DIVISION CHIEF - DR. J.K. PARRY

CONTENTS

CONTENTS (cont'd)

CONTENTS (cont'd)

CONTENTS (cont'd)

CONTENTS (cont'd)

1. INTRODUCTION

In September 1980, the Commission approved a reorganisation of Physics Division, Engineering Research Division and Instrumentation and Control Division to form two new research divisions to be known as Applied Physics Division and Nuclear Technology Division.

The Applied Physics Division will be responsible for applied science programs, particularly those concerned with nuclear techniques. The Division is organised as four sections with the following responsibilities:

(1) Nuclear Applications and Energy Studies Section. Program includes studies in nuclear physics, nuclear applications, ion implantation and neutron scattering.

(2) Semiconductor and Radiation Physics Section. Studies in semiconductor radiation detectors, radiation standards and laser applications.

(3) Electronic Systems Section. This includes systems analysis, digital systems, instrument design, project instrumentation and instrument maintenance.

(4) Fusion Physics Section. This covers work carried out by staff currently attached to university groups.

The format in this progress report, which reports on the period October 1, 1980, to June 30, 1981, has been chosen to conform with the organisational structure outlined above.

2. NUCLEAR APPLICATIONS AND ENERGY STUDIES

2.1 Nuclear Physics

2.1.1 Nuclear safeguards (J.W. Boldeman)

A program of research and development has been initiated as part of the Australian Government's three year program of assistance to the International Atomic Energy Agency. The first project within this program is the development of a gas phase monitor to determine ^{235}U enrichment in the output of gas centrifuge plants. The principle of operation is as follows. The total uranium content of a UF_6 gas sample is determined by a measurement of the attenuation of the 60 keV gamma rays from an ^{241}Am source in passing through the sample volume. The measurement is accomplished with a NaI detector. The ^{235}U concentration in the same sample is obtained by counting the 185.7 keV gamma rays from the decay of the ^{235}U in the same NaI detector. A comparison of the two count rates gives the ^{235}U enrichment after calibration of the detection system with suitable gas standards. The feasibility of the method has already been established by

previous work[1,2].

2.1.2 Measurement of neutron fission cross section for ^{230}Th (J.W. Boldeman, R.L. Walsh)

Measurements of σ_{nf} for ^{230}Th for E_n = 750 to 735 keV were made in order to check the data of Blons et al.[3] in this energy region and to verify the energy scale and resolution of our previous measurements of the fission fragment angular distribution for neutron fission of ^{230}Th[4]. Neutrons were generated by the ^{7}Li(p,n) ^{7}Be reaction. The fission detector was a fast ionisation chamber, containing a single ^{230}Th electroplated target of thickness 1 mg cm^{-2} at 9 cm from the Li target. The neutron flux was monitored by a long counter. The neutron energy was increased in steps of 2 keV for each run. The neutron energy spread for each run was ±1.5 keV.

The results indicate that the 3 MeV Van de Graaff accelerator is accurate in proton energy to better than 1 keV. The shape of the fission cross section (Figure 1) also confirmed the calculated energy resolution and verified the stated resolution of the fission fragment angular distribution measurements.

2.1.3 A laboratory mass asymmetry in the mass division of ^{230}Th following neutron fission at 710 keV

(D.W. Lang, J.W. Boldeman, R.L. Walsh, I.F. Senior)

Central to any description of the fission process is a model of the potential energy of the nucleus as a function of deformation. The most successful model for ^{230}Th(n,f) requires a triple-humped fission barrier[4]. The saddle point is located near a shallow minimum in the deformation energy associated with a splitting of the outer portion of a double-humped barrier. According to the model, the nucleus can be pictured as pear-shaped with rotational symmetry about the long axis. Consideration of timescales suggests that once the nucleus leaves the saddle point, a number of quantum numbers are 'frozen in' and this is supported by success in accounting for the observed angular distributions of fission fragments.

In turn, it could be expected that a pear-shaped nucleus would fission

---

1) Greenwood-Smith, R. (1971)-WSCN/103

2) Strittmather, R.B., Leavitt, J.N. and Slice, R.W. (1980) - LA-8657-MS

3) Blons, J., Mazur, C., Paya, D., Ribrag, N. and Weigmann, H. (1978) - Phys. Rev. Lett. 41:1289

4) Boldeman, J.W., Gogny, D., Musgrove, A.R. de L. and Walsh, R.L. (1980) - Phys. Rev. C. 22:627.

with the light fragment associated with the 'stalk' end of the pear. An experiment is in preparation with the object of confirming this. Difficulties would be expected on a nuclear scale in preparing a pear-shaped object. By definition it would have no reflection symmetry along its axis. The state with the stalk in one direction would have the same energy as its mirror image with the stalk in the opposite direction. The symmetry of nuclear interactions would in general require that the actual states observed would be two possible mixtures of the simplest states pictured. These two mixture states have a symmetry under reflection and usually are separated in energy.

In the case of the compound nucleus ^{231}Th, the separation is believed to be less than the decay width of the state, so it should be possible to prepare a state of the nucleus at an intermediate energy and to define a preferred direction for the stalk of the pear and hence for the emission of the light fragment.

Using neutrons polarised perpendicular to the beam direction, the asymmetry occurs in a line perpendicular to the direction of polarisation. However, the direction of the maximum asymmetry effect is unknown.

The fission detector system has been constructed and a thin ^{230}Th target is being prepared by electrospraying.

2.1.4 Mass resolution correction in double-energy fission measurements (D.W. Lang, R.L. Walsh)

Our measured mass yield curves for ^{252}Cf(sf)[5] and ^{239}Pu(n,f)[6] have been corrected for mass resolution by three methods:

(i) a polynomial inversion operator method;
(ii) a moment reduction operator method[7]; and
(iii) a conjugate gradient iterative method[8].

For methods (i) and (ii), the resulting yield curves for ^{239}Pu(n,f) contain shoulders at masses 106 and 134 amu (Figure 2) which have not been reported by other authors. Figure 3 shows the final yield curve using method

---

[5] Walsh, R.L. and Boldeman, J.W. (1977) - Nucl. Phys. A276:189.

[6] Walsh, R.L., Boldeman, J.W. and Elcombe, M.M. (1979) - Proc. IAEA Symp. Physics and Chemistry of Fission, Jülich, Vol. 2, p. 129.

[7] Terrell, J. (1962) - Phys. Rev. 127:880.

[8] Lang, D.W. (1977) - AAEC/E398.

(iii), after five iterations. The structure at 106 and 134 amu is again apparent. As a check on this structure, further tests were performed using the iterative method. In a series of runs:

(a) the shoulders were found to be visible with three iterations and to develop further as part of a complicated overall structure when ten iterations were performed;

(b) the shoulders appeared just as swiftly if a constraint was applied to keep the spectrum non-negative but other complicated structure developed much more slowly;

(c) when raw data from Neiler et al. [9] were used as input and were unfolded, these shoulders did not emerge; and

(d) when test raw data were generated using a double Gaussian mass distribution, unfolding discrepancies were speedily reduced to one tenth of those for experimental data and no such features as shoulders appeared.

It is concluded that the shoulders at 106 and 134 amu represent a genuine difference in the data reported in refs. [6] and [9]. It should be noted that calculations of the expected fine structure positions for ^{239}Pu(n,f) by Unik et al.[10] from the masses of even-Z fragments[11] do show that mass yield fine structure is expected at masses 106 and 134 amu.

It is further instructive to compare the unfolded spectrum with the raw data and to calculate the residual discrepancies. The unfolded spectrum has been subtracted from the raw data and the difference plotted in Figure 4. Applying the resolution broadening to the unfolded spectrum gives the predicted yields. The residual discrepancies in the fit to the data are obtained by subtracting the predicted yield from the raw data. The residual discrepancies are also shown in Figure 4 and are seen to be about one-fifth of the magnitude of the unfolding corrections which in turn are about one-tenth of the maximum yields.

2.1.5 ^{252}Cf fission neutron spectrum (J.W. Boldeman, J. Fallon)

The fission neutron spectrum from the spontaneous fission of ^{252}Cf has

---

[9] Neiler, J.H., Walter, F.J. and Schmitt, H.W. (1966) - Phys. Rev. 149:894

[10] Unik, J.P., Gindler, J.E., Glendenin, L.E., Flynn, K.F., Gorski, A. and Sjoblom, R.K. (1973) - Proc. 3rd IAEA Symp. Physics and Chemistry of Fission, Rochester, N.Y. 2:19.

[11] Thomas, T.D. and Vandenbosch, R. (1964) - Phys. Rev. 133:B976.

been measured previously for the energy range 1 to 15 MeV[12]. This work has been extended to cover the energy range 0.1 to 1.0 MeV. A series of measurements has been made for this range using the original recording system but substituting an enriched ^{6}Li glass scintillator (0.5 mm thick) in place of the previous neutron detector. A considerable amount of data has been generated, but the analysis is still unsatisfactory. The problem is the scattering of neutrons in the detector assembly (photomultiplier tube, etc.) back into the detecting volume of the glass scintillator. Because of the short flight path of the experiment (measurements at 40, 60, 80 cm), the backscattered neutrons are apparently shifted substantially lower in energy. To correct for this problem the detector response is being measured for a large number of neutron energies using mono-energetic neutron beams generated with a pulsed 3 MeV Van de Graaff accelerator.

2.1.6 Collaborative experiments with CBNM at the Geel Electron Linear Accelerator (B.J. Allen, A. Brusegan*, G. Rohr*, R. Shelley*, T. van der Veen*)

(a) High resolution neutron capture cross sections of ^{54}Fe

High resolution capture cross section measurements of the isotopes of iron have continued with an enriched sample of ^{54}Fe obtained on loan from Oak Ridge National Laboratory.

The oxide sample was packed in a 0.3 mm thick aluminium container of 8 cm diameter and placed at a neutron flight path distance of 60 m. Neutron capture gamma rays were detected with two deuterated benzene (C_6D_6) detectors and off-line pulse height weighting of detected gamma rays was used to ensure that the capture efficiency was independent of the resonance gamma ray spectra. The linac GELINA was operated at 800 Hz with a pulse width of 4 ns.

Neutron flux measurements were made with a 0.5 mm ^{6}Li glass in the transmission mode, and with a boron slab viewed by two C_6D_6 detectors. The absolute normalisation of the neutron flux was obtained by means of the 1.15 keV resonance in ^{56}Fe. The parameters of this resonance have been accurately measured in transmission experiments.

The ^{54}Fe data are of better quality than earlier measurements at ORELA

---

*Central Bureau for Nuclear Measurements, Geel, Belgium

[12] Boldeman, J.W., Culley, D. and Cawley, R. (1979) - Trans. Am. Phys. Soc. 32:733

(Allen et al. 1977[13]) in that the sensitivity of the detector system to resonance scattered neutrons is much reduced, and the flight path is half as long again. Although the sensitivity of the GELINA capture system has not yet been investigated in detail, a lower effect is expected because of the open beam geometry and the absence of fluorine in the scintillator. Measurements of the neutron sensitivity are planned by observing gamma ray yields from resonances in Al and Si with large neutron scattering widths.

A striking feature of the ^{54}Fe data is the asymmetry observed in the s-wave resonances of 130, 147, 174 and 190 keV. These results confirm the asymmetries reported by Allen et al. (1978)[14] for the ORELA data which were interpreted as interference between the single particle or valence components of s-wave resonances with large neutron widths. The effect is so significant that a multi-level, multi-capture channel analysis will be required.

At present, analysis of the ^{54}Fe data is proceeding using both area and shape fitting programs for the determination of resonance capture widths. The latter code, based on an s-matrix calculation of the scattering cross section, has recently been adapted to the high resolution requirements of the GELINA measurements.

(b) An investigation of the neutron capture mechanism in ^{88}Sr

The asymmetric capture resonances observed in ^{54}Fe have been interpreted as a manifestation of the valence neutron capture mechanism in the 3s strength function region of the N = 28 closed neutron shell. A similar effect is expected when the 3p single particle state becomes unbound at the N = 50 magic neutron number. Earlier capture measurements at ORELA (Boldeman et al. 1976[15]) showed a strong correlation between the p-wave reduced neutron widths and the corresponding radiative widths. It is therefore expected that interference effects may also be observed in the capture channels for the strong p-wave resonances near 300 keV and 550 keV.

A $Sr(NO_3)_2$ sample, highly enriched in ^{88}Sr, was loaned by Oak Ridge National Laboratory to the AAEC. The resonance capture yield has been measured from 0.2 to 600 keV using C_6D_6 detectors at the 60 m station. The yields in the

---

13) Allen, B.J., Musgrove, A.R. de L. and Boldeman, J.W. and Macklin R.L. (1977) - Nucl. Phys. A283, 37.

14) Allen, B.J., Musgrove, A.R. de L. and Bertram, W.K. (1978) - Phys. Lett. 72B:323

15) Boldeman, J.W., Allen, B.J., Musgrove A.R. de L., Macklin, R.L. and Winters, R.R. (1976) - Nucl. Phys. A269:397.

vicinity of 300 keV appear to be asymmetric for the strong p-wave resonances. However, statistics are inadequate above 500 keV. High bias data were also recorded in an endeavour to obtain the ground state partial capture cross section. This would provide a more direct comparison with the valence model.

A moderated neutron target was used for the present measurement. An unmoderated target would give a much higher neutron flux above 500 keV, but may result in severe gamma-flash problems. This latter option is under investigation.

2.1.7 Fast neutron capture gamma-ray spectra in ^{88}Sr, ^{139}La and ^{141}Pr (B.J. Allen, F.Z. Company,* J.N. Mathur*)

The neutron capture mechanism has been investigated in the closed shell nuclides ^{88}Sr (N = 50) and ^{139}La, ^{141}Pr (N = 82) by the measurement of capture γ-ray spectra for 10-1000 keV neutrons.

Measurements were made at the AAEC's 3 MeV Van de Graaff using a 2 MHz pulsed proton beam with $\sim$3 ns width. Neutrons were produced by the $^{7}Li(p,n)$ reaction and capture γ-rays were detected by a well-shielded 20 x 15 cm NaI detector. Measurement, data reduction and analysis techniques were similar to those described by Barrett et al. (1977)[16].

Neutron capture γ-ray spectra were measured for neutron energies between 345-1025 keV for ^{141}Pr and 180-270 keV for ^{139}La. Neutron energy spread in the ^{7}Li target was $\sim$25 keV so capture spectra are averaged over $\sim$100 resonances in Pr and 225 in Li.

The high energy γ-rays are seen to increase in energy for high neutron energies, confirming the primary nature of the radiation. After line shape analysis of the capture spectra, the data were divided by $n.E_{\gamma}^{3}$ where n is the number of final states per 0.1 MeV interval (Groshev et al. 1968)[17]. The average neutron energy was then subtracted to obtain reduced spectra for comparison with the statistical model and with the high resolution thermal data.

The observed γ-ray strength per final state generally shows a strong

---

*University of Wollongong

16) Barrett, R.F. et al. (1977) - Nucl. Phys. A278:204

17) Groshev, L.V. et al. (1968) - Nucl. Data Tables 5:1

high energy component, but this disappears when the E_γ^3 factor is introduced. Overall, the spectra are consistent with the statistical model (for primary γ-rays $I_\gamma(n.E_\gamma^3)^{-1} \sim$ constant), but exhibit marked fluctuations which cannot be attributed to the spectrum averaging method.

In the case of ^{88}Sr, strong initial state correlations for $P_{1/2}$ and $P_{3/2}$ resonances have been reported in neutron capture cross section measurements (Boldeman et al. 1976)[18], and estimates of valence capture accounts for a large fraction of the observed radiation widths. Therefore it is of considerable interest to measure γ-ray spectra, particularly in the 300 keV region, where the valence component is expected to be largest.

According to Boldeman et al.[18], the largest valence contributions to resonance capture are at 321 and 287 keV and it is in these regions that transitions to the $d_{5/2}$ and $s_{1/2}$ states but not $d_{3/2}$ states dominate the capture spectrum in agreement with valence expectations. Nevertheless, strong transitions to the weak $\ell_n = 2$ states at $\sim$3 MeV, which dominate the spectra at 400-500 keV, suggest an important role for an additional non-statistical capture mechanism.

2.1.8 $^{175}Lu(n,\gamma)^{176m}Lu$ cross sections (B.J. Allen, G.C. Lowenthal, J.W. Boldeman)

Four irradiations were made at a proton energy of 25 keV above the ^7Li (p,n) threshold. The flux weighted ratio of the Lu isomer and Au capture cross sections was found to be $\langle\sigma^m_{175}\rangle/\langle\sigma_{197}\rangle = 1.654 \pm 0.076$ (SD). This result is 26 per cent higher than the Beer and Käppeler (1980)[19] value, but 14 per cent lower than that of Allen et al. (1981)[20]. This latter difference is well outside the 4 per cent uncertainties for both measurements.

The isomeric capture cross section at 30 ± 10 keV is then $\langle\sigma^m_{175\ 30}\rangle = 958 \pm 58$ mbarn and the isomeric branching ratio $B^m = 0.78 \pm 0.10$.

Using our new value for B, we obtain a negative age for s-process synthesis. An alternative interpretation, first suggested by Clayton (1963)[21], is that thermalisation of the ^{176}Lu ground and isomeric state populations occurs in the stellar environment. The effective half-life of ^{176}Lu is obtained from the Boltzmann equation and reduces to

$$t_- = t_{1/2}\ (2J_o + 1)/(2J_1 + 1)\ \exp\ (E_1 - E_o)/kT = 0.14\ y$$

---

18) Boldeman, J.W. et al. (1976) - Nucl. Phys. A269:397

19) Beer, H. and Käppeler, F. (1980) - Phys. Rev. C 21:534

20) Allen, B.J. Lowenthal, G.C. and de Laeter, J.R. (1981) - J.Phys.G., 7:1271

21) Clayton, E. (1963) - private communication

for $J_o = 7$, $j_1 = 1$, $E_1 = 127$ keV, $t_{1/2} = 3.64$ h and kT = 30 keV. The changed half-life results from the weak population of the isomeric state (0.3 per cent at 30 keV) in thermal equilibrium with the stellar environment.

The s-process branch at ^{176}Lu to ^{176}Hf is defined as

$$f_- = 1 - (N_s\sigma)_{^{176}Lu}/\langle N_s\sigma\rangle_{176} = 0.61 \pm 0.07$$

and is seen to be substantially less than our isomeric branching ratio. Consequently, the population of the isomeric state must be reduced significantly in less than 3.64 h to reduce the isomeric decay rate. It is unlikely that this effect could be achieved directly by photo de-excitation ($\Delta J = 6$), but photon inelastic scattering and Coulomb excitation processes could establish a thermal equilibrium by electro-magnetic linkage to higher excited states. Recently Ward (1980)[22] found that enhanced decay rates could occur from Coulomb collisions with the ion plasma in the stellar environment. From analytic approximations the resulting de-excitation rates are strongly dependent on the A and Z of the target and projectile, stellar temperature, multipole order and type and energy of the transition. For ^{176}Lu, enhancement could occur above 4.10^8 K for helium burning and above 10.10^8 K for carbon burning. Coulomb enhancement of indirect transitions, linked through higher lying states, may prove to be even more significant than direct transitions in determining the thermal equilibrium rate.

2.1.9 3 MeV Van de Graaff accelerator (J. Fallon, I. Senior)

Total experiment hours of the accelerator for the nine months to June 1981 were 1416. There was no time lost other than for routine maintenance which occupied 554 hours. Time used by each experimental category is shown in Table 1.

Base pressure

Following problems last year when many ion sources cracked and maintaining good vacuum was difficult, the accelerator has now run for nine months with base pressures of approximately 0.15 mPa. Good ion source performance can now be obtained with gas settings as low as 0.5 mPa.

Terminal performance

Good pulsing (2 ns, 3 μA on target, energies to 3 MeV) is readily available

---

22) Ward, R.A. (1980) - Astronomy and Astrophysics (in press)

provided that the ion source and deflection chamber have not previously run for an excessive number of hours. This time is dependent on the type of ions accelerated and the current drawn from the ion source. Stable d.c. beams as low as 1 μA on the beam stop and only several nano-amps on the target have been run and maintained for several hours. The accelerating tube has now been in service for >5500 hours and requires no conditioning for terminal voltages up to 3 MV.

2.1.10 Computer replacement

The main data acquisition system for accelerator and reactor experiments has been replaced by an LSI 11/23 with disk storage and two LeCroy 3500 remote terminals. The earlier system involved coupled PDP7 and PDP15 units and these are being phased out as the new system becomes fully operational. At a short ceremony on 24 June 1981, the PDP7 was formally handed back to Digital Equipment Aust. Pty Limited for use as a prime exhibit in their new computer museum at Chatswood, NSW. The PDP7 was the first unit of its type in Australia and was used for many innovative developments, clocking up 111 577 hours of operation in its 15 years of use.

2.2 Nuclear Applications

2.2.1 Hydrogen profile measurements (N. Livick†, D.D. Cohen*, P. Duerden, G. Harding†)

The hydrogen profile in sputtered solar surfaces (C or Cu) is being measured by analysis of protons, elastically scattered from the profile by an incident alpha-particle beam. A beam of 2.5 MeV α particles collimated by a 0.5 mm slit is incident to the target. The elastically recoiled protons are detected with a surface barrier detector, that is itself collimated by a 0.5 mm slit. An aluminium foil (11 μm thick) is placed in front of the detector to stop scattered incident α particles.

Typical hydrogen profiles measured with different angles of incidence of the α particle to the surface and with different emergent angles to the detector are shown in Figure 5. It has been found that the best depth resolution for the measurement is obtained with 5° emergent glancing angles to the surface. For incident/emergent angles smaller than 5°, the straggling of the α particles and the recoil proton makes the depth resolution worse. Depth resolutions of

---

*Australian Institute of Nuclear Science and Engineering

†University of Sydney

5 nm have been found for hydrogen in carbon surfaces on Cu substrates.

2.2.2 Glancing angle measurements of oxygen depth profiles

(J.R. Bird, P. Duerden, D.D. Cohen*, G.B. Smith††, P. Hillary††)

The $^{18}O(p,\alpha)^{15}N$ reaction is much used for oxygen depth profiling and the depth resolution that can be achieved can be considerably improved by using glancing angle techniques.

An 840 keV proton beam, collimated to 1 mm diameter, is incident on a sample mounted on a goniometer located at the centre of a 20 cm diameter target chamber. A surface barrier detector can be rotated to select different reaction angles. It is collimated with a 1 mm wide slit and there is a 2 $\mu g/cm^{-2}$ anodised Mylar foil placed in front of the detector to remove scattered protons. We have used a variety of reactions and alpha-particle emergence angles with Ta_2O_5 reference samples. The effect of variation of emergence angle is shown in Figure 6 where the reaction angle is constant at 65°.

It is seen that there is considerable advantage in using forward angles for the study of these oxide layers. As in other glancing angle studies, surface flatness, smoothness and absence of contamination are important for obtaining satisfactory results.

A study of oxide depth profiles on chrome black surfaces is being carried out in association with the New South Wales Institute of Technology. A report of the preliminary studies was presented at the 5th International Ion Beam Analysis Conference held in Sydney, February 1981.

2.2.3 Computer simulation of X-ray spectra (E.J. Clayton)

A computer program SOXS (synthesis of X-ray spectra) has been written to generate theoretical PIXE spectra for a wide range of experimental conditions. It is used to provide insight into the analysts' usual questions: "What are the minimum detection limits? Will element interference be severe? How does the target matrix composition affect the X-ray yield of a given element?" SOXS uses input trace element concentrations to produce a simulated PIXE spectrum. In either thick or thin targets, for element concentrations from $\mu g\ g^{-1}$ to 100%, the X-ray yield of an element in a sample can be estimated, given its concentration[23]. This yield can be converted to a complete set of element characteristic X-ray peaks. The basic Gaussian representation of the peaks can be distorted by adding low energy tailing or step functions. Adding the characteristic X-ray peaks for

---

*Australian Institute of Nuclear Science and Engineering
††New South Wales Institute of Technology
23)Clayton, E., Cohen, D.D. & Duerden, P.(1981) - Nucl.Instrum.Methods 180:541

each element to one of the libraries of standard backgrounds gives a complete spectrum. Any detector geometry and filter condition can be simulated allowing detailed experiment planning and feasibility decision making. Careful design of filters to transmit X-rays preferentially in predetermined portions of the X-ray spectrum optimises experimental running conditions. A filter providing such flexibility is the pinhole filter. By adjusting the thickness of the filter and the size of the pinhole, one can balance the contribution to the complete spectrum of both heavy and light elements with their disparate X-ray yields. Figure 7 shows a simulated spectrum from obsidian, and was used during the design of a pinhole filter.

2.2.4 Uncertainties in theoretical thick target yields (E.J. Clayton)

The proton induced X-ray yield for an element in some matrix depends on many processes. As well as the ionisation cross section, proton stopping power and X-ray attenuation effects, uncertainties in experimental measurement, both in the efficiency of detecting X-rays and in collecting the incident proton charge, have an influence on the accuracy with which thick sample PIXE analysis can be undertaken. A survey of the various processes occurring in proton induced X-ray emission has been made in the past year. Theoretical thick target yields using currently accepted best values were compared with experiment for various thick targets. In summary, a first estimate on the uncertainty of thick target yields is in the range 10 to 15%.

Table 2 shows measured and literature concentrations for the U.S. Geological Survey standards BCR1 and W1, where the measured values were obtained from the theoretical yield curve[23]. Figure 8 shows the analysis of a multi-element cocktail in graphite. Over 40 elements, each with a nominal concentration of 200 μg g^{-1}, were incorporated into a graphite matrix. In this figure, 26 elements, yielding both K and L line X-rays, are shown. Analysis of this cocktail gave an average difference between nominal and estimated yield of 7%.

2.2.5 M-shell X-ray emission for determination of the low energy efficiency of Si(Li) detectors (D.D. Cohen, AINSE)

In a previous paper[24] a simple five-parameter radially dependent photopeak efficiency model for semiconductors or detectors was developed. The validity of this model was verified to ±3% over the X-ray energy range 5 to 60 keV using calibrated X-ray sources. This model, however, is not limited to energies above 5 keV; explicit expressions for the efficiencies in some cases were obtained for energies as low as 0.2 keV.

---

[24] Cohen, D.D. (1980) - Nucl.Instrum.Methods 178:481

Extensive work has been done on L X-rays produced by proton and He^+ ion bombardment of both thin and thick targets in the atomic number range $66 \leq Z \leq 92$. The Lα X-rays for these targets cover the X-ray energies $6.5 \leq E_x \leq 13.6$ keV, where Si(Li) detector efficiencies can be easily measured by standard source techniques. Mα X-rays for these targets lie between $1.2 \leq E_x \leq 3.2$ keV where accurate efficiencies are hard to obtain. Several theories exist to predict the L and M shell ionisation cross sections σ^I [25] and these can differ in absolute magnitude by significant amounts. However, the theoretical ratio $R_{ML} = \left[\sigma^I_M/\sigma^I_L\right]_{theory}$ is reasonably consistent for most theories in our projectile energy range of interest (1 to 3 MeV). This ratio can easily be compared with the experimental value obtained from the ratio of the measured M and L X-ray counts and the detector efficiencies in the 1 to 3 keV region calculated.

The ratios of M to L, X-ray production rates for He^+ bombardment of both thin and thick targets from Dy through to U have been used to measure the efficiency of a thin window (8 μm), high resolution (142 eV at 5.9 keV) ORTEC Si(Li) detector in the 1 to 5 keV energy region.

Figure 9 is a typical X-ray spectrum for 2.6 MeV He^+ ion on thick W. The M X-rays are clearly seen sitting in the secondary electron bremsstrahlung background, while the L X-rays, although nearly two orders of magnitude smaller, are still well resolved and sit in an essentially zero background. The relevant peak areas were extracted by first removing the background and then fitting Gaussians to the peaks.

Figure 10 shows the measured efficiency for our Si(Li) detector over the entire energy range 1 to 60 keV. The crosses represent efficiencies calculated previously using standard sources [24] and the open circles represent results using helium induced M X-ray emission (HIXE). For the HIXE results, two points are plotted at each energy with error bars representing the thin and thick target results. Each point is the mean for all results taken over the projectile energy range 1 to 3 MeV.

The solid and chained curves are a fit to the data using the radially dependent photopeak efficiency model [25]. The chained curve shows zero ice thickness on the front of the detector. The solid curve is a fit to the data giving a 13 μm thick layer of ice on the detector front face. The dashed lines either side of the solid curve represent the ±3σ standard deviation confidence interval about this fit. The discontinuity at 1.84 keV is a consequence of the Si K absorption edge and is produced by the 0.3 μm thick silicon dead layer on

---

[25] Brandt, W. and Lapicki, G. (1979) - Phys. Rev. A20:465

the front face of the detector. Slight discontinuities between 2 and 4 keV are similarly produced by the Au M_1 to M_5 absorption edges as a consequence of the 0.02 um thick evaporated gold contact on the detector front face.

The M shell fluorescence technique has been used successfully to monitor this ice build-up in the detector as a function of time over many months. Figure 11 shows the ice thickness versus time, as well as the corresponding decrease in detector efficiency for Al Kα X-rays of energy 1.486 keV as the ice thickness increases.

The detector crystal has been warmed up, pumped and the ice removed, returning its efficiency to its original state with no loss in resolution.

2.2.6 Archaeometry (P. Duerden, J.R. Bird, W.R. Ambrose*, B.F. Leach†, O.S. Rye*)

The extensive PIXE and PIGME measurement programs on South West Pacific obsidian and Papua-New Guinea pottery artefacts have continued and were reported upon at the 5th International Ion Beam Analysis Conference[26].

A notable result of recent measurements has been the sourcing of obsidian samples found in Misisil, a large hill top cave in the West New Britain province of Papua-New Guinea. The obsidian samples shown to come from the Talasea region were associated in the cave with wood charcoal that has been dated at $11\ 300^{+1200}_{-1100}$ B.P.

2.2.7 Proton induced decoration (J.R. Bird, R.W.T. Wilkins††, A. Rose)

Additional measurements have been made of optical absorption during proton irradiation of halite and synthetic NaCl crystals. The results show that the rate of growth of absorption at 580 nm (usually attributed to the formation of colloid particles) peaks at a temperature in the neighbourhood of 170° C (Figure 12) after an initial saturation which is a linear function of 1/T (Figure 13). This behaviour, which has also been reported for electron irradiation is not directly correlated with the appearance of colour bands which decorate dislocations in the natural crystals.

---

*Department of Prehistory, Research School of Pacific Studies, Australian National University, Canberra, A.C.T.

†Anthropology Department, University of Otago, Dunedin, New Zealand

††CSIRO Division of Mineralogy, North Ryde, NSW

26) 5th Int. Conf. Ion Beam Analysis, Sydney, 16-20 Feb. 1981

26a) Swyler, K.F., Klaffky, R.W. and Levy, P.W. (1979), Brookhaven National Laboratory, New York, U.S.A. - 26917.

Decoration is not observed in halite which is annealed for one hour at 500° C before irradiation, unless the crystal is again deformed between annealing and irradiation. Comparable behaviour is not observed for synthetic crystals. It is apparent, therefore, that the presence of suitable impurity concentrations in natural crystals enables proton induced decoration of glide bands and other features also present in these crystals.

2.2.8 International Conference

The 5th International Conference on Ion Beam Analysis was held at the University of New South Wales on 16-20 February 1981. Staff of Applied Physics Division at Lucas Heights were extensively involved in the organisation of the Conference, as editors of the Proceedings and as co-authors of nine papers presented at oral or poster sessions. Two International Workshops were held in conjunction with the Conference and additional papers were presented at these events. Approximately 80 overseas scientists attended the Conference and Workshops and many visited Lucas Heights for discussions on current programs. It was a great pleasure to have B.R. Appleton of Oak Ridge National Laboratory (ORNL) attached to Applied Physics Division for three months overlapping the period of the Conference.

2.2.9 Fluorine in coal (E. Tiller*)

A 2.5 MeV proton beam has been used for initial measurements of proton induced gamma rays from fluorine in coal. An ultra high vacuum chamber is differentially pumped using an in-line cold trap and samples are mounted on a holder which permits a Ge(Li) detector to be placed as close as possible to 0° with respect to the incident proton beam.

Reference samples (CaF_2 in an Al_2O_3 matrix; graphite for background determination) and pressed powdered coal have been used and good gamma-ray spectra obtained which are now being processed.

2.2.10 Moata (D.J. Wilson, T. Wall)

Moata reactor operated for 470 hours with a total energy production of 21.4 MWh. Uranium ore assay, neutron radiography and the irradiation of minerals and SYNROC used most of the time, but other applications involving Applied Physics Division, other divisions, and university workers, included:

- Bioassay of tissue materials - hair, urine and blood
- Plutonium particle size analysis
- Molecular breakdown of gases at high radiation doses

*Darling Downs Institute of Advanced Education, Queensland

New control and safety channels (from the critical facility) have been installed and are being tested and compared with the current installed instrumentation. If the new channels prove satisfactory in all areas of control and safety, it is expected that they will replace the older channels.

2.2.11 Bioassay (D.J. Wilson)

Further neutron irradiation experiments have been made to determine the effect of age and sex on the uptake of uranium by hair (using mice) and calculations have been carried out to determine the distribution of fission tracks inside and outside a thin cylinder (of hair) to determine the absolute fission rate of the uranium contained by the hair.

2.2.12 Uranium assay (T. Wall)

The number of samples analysed (from 12 different sources) between 1 October 1980 and 30 June 1981 was 4443. Since the uranium analysis service commenced operation, 50 400 samples have been analysed, of which 25 355 have been forwarded by non-AAEC organisations.

2.2.13 Soil moisture studies (D.J. Wilson)

Calculations have continued to determine the effect of resonance capture, the geometry of the probe and the effect of using different types of neutron source (Ra-Be, Ac-Be, Po-Be, Am-Be, Pu-Be) on the analysis of soil moisture measurements. The influence of the size of the source (that is, the amount of Pu in a Pu-Be source) on the neutron spectrum and the response of the detector has been examined.

The variation of the depletion response with each of the soil parameters, density, absorption cross section and scattering cross section, has been fitted to polynomial expressions and a simple computer program has been written to solve the resulting empirical relationship connecting a normalised count rate from the probe with the water content and known parameters of the soil.

Comparison of calculated with measured results for two different soils with widely differing parameters, after normalisation at one point, shows that the program calculates the moisture content to within 5% over the whole range.

Further calculations are being carried out and planned to assess the possible use of moisture probes in coal or oil-shale deposits and to determine the corrections necessary to take account of bore hole linings, pebbles and voids and the proximity of the soil surface.

2.2.14 Particle track techniques (T. Wall, W.R. Ellis*)

Solid state nuclear track detectors have been used to determine the identity and amount of actinide contamination at a site formerly used for the safety testing of nuclear material. Results were obtained by using heterogeneous soil samples. The techniques of particle identification and sizing are apparently as successful for this medium as those developed elsewhere for aerosol contamination analyses using particulate filters. Figure 14 shows the sizes of PuO_2 particles obtained by taking fission and alpha track replicates of soil samples from the Maralinga test site, South Australia.

The replicates were scanned with an optical microscope to locate sites of particulate contamination and the number of tracks observed was related to the mass and hence the size of the particulate causing the contamination. By using a combination of fission track (muscovite mica) and alpha track (CR39) detectors, it was possible to discriminate and quantify both ^{239}Pu and natural uranium.

The CR39 detector efficiency for alpha particles from ^{239}Pu was also measured by mapping the track image of individual particles. The track density (Figure 15) may be modelled to a simple relationship involving the height of the particle above the detector surface and the track image radius. This enabled the critical angle, θ_c, at which tracks are just retained by the detector, to be measured and hence an estimate of the detector efficiency.

2.3 Ion Implantation

2.3.1 Ion implantation - experimental equipment (M.J. Kenny, H.G. Broe, D. Stevenson)

Support has been obtained from the National Energy Research, Development and Demonstration Council (NERDDC) for up to $54 000 for major equipment purchases for the ion implantation-photovoltaics project. This will enable purchase of a high current solid feed ion source and components for the ultra high vacuum system. The primary use of this equipment is for implanting silicon wafers for photovoltaic cell fabrication. The project aims to use the solid feed ion source and to produce arsenic or phosphorus beams to implant silicon wafers directly without carrying out mass analysis of the beam. Damage caused by implantation is removed by laser annealing and contacts added to produce a solar cell. These cells are then evaluated against those manufactured by more complex methods.

---

*Environmental Science Division

Medium current 25 kV implanter

An ion implantation facility has been set up to produce ion beams from gases. It uses a duoplasmatron ion source enclosed in a high voltage cage which can be operated at up to 25 kV above ground potential. Acceleration is across an ultra high vacuum ceramic insulator and samples are mounted within a stainless steel chamber pumped by a turbomolecular pump. Pressure in this chamber is <0.1 mPa. Beams have been obtained for H_2, N_2 and Ar gases with currents in excess of 1 mA. Stable operation is best obtained with lower currents as shown in Table 3. This ion source can, in principle, be used to obtain beams from almost any gas. Since no mass analysis is used, various components are present in the beam, e.g. H^+, H_2^+, H^+-H_2, when hydrogen is used. A current of 100 μA on 1 cm^2 area can implant 6 x 10^{14} ions cm^{-2} s^{-1}. Typical implant doses vary from 10^{15} to 10^{17} cm^{-2}, so implant times are relatively short.

High current 50 kV implanter

An order has been placed for a Freeman type solid feed ion source capable of producing ion currents in excess of 6 mA. Specifically, phosphorus or arsenic ion beams will be used for implantation into silicon; however, a wide range of other ion beams will also be available. The ultra high vacuum system for this implanter has been assembled and tested. The helium cryopump has pumped the system to a pressure below 1.0 μPa. Key features of the photovoltaic project are the elimination of the mass analysis system and the use of clean, ultra-high vacuum system. The experimental layout is shown in Figure 16.

2.3.2 Depth distribution of dopants in arsenic implanted silicon

(M.J. Kenny, M.D. Scott, A. Rose)

In the manufacture of silicon solar cells, relatively shallow doping (∿0.04 μm) is required. Arsenic ions were implanted into <111> silicon wafers at an energy of 30 keV and a dose of 10^{15} ions cm^{-2}. The surface structure of the silicon was then studied using Rutherford backscattering (RBS) and channelled 2 MeV He^+ ions. Two surface barrier detectors were used: one at 170° to locate the channelling position, the other at 95° to give superior depth resolution. It was found that the implanting had damaged the Si crystal down to a depth of 0.038 μm.

A pulsed ruby laser (energy 1.5 J cm^{-2}, pulse width 25 ns and spot size 7 mm diameter) was used to remove the crystal damage and restore electrical activity. After annealing, the backscattering measurements were repeated and it was found that almost all the damage had been removed. Figure 17 shows backscattering spectra for a random alignment and for channelling along the

<111> axis before and after laser annealing. The spectrum in the annealed case is virtually identical to that for pure (unimplanted) silicon. After annealing, the arsenic peak counts were reduced to 10±1% of the damaged or random peak area, demonstrating 90% substitutionality of the As dopant. Also shown on Figure 17 is the calculated spectrum for a sample consisting of 1 nm carbon impurity, 8 nm of damaged silicon, 18 nm of 99.3% Si, 0.7% As, 12 nm of damaged silicon and 1 nm of crystal silicon. It is seen to be in excellent agreement with the observed spectrum.

2.3.3 Laser annealing (A. Rose, D. Stevenson)

Pulsed laser

A Q-switched ruby laser capable of producing high power (100 MW cm^{-2}) pulsed beams is being used for semiconductor surface studies. During the latter part of 1980, this laser was used for annealing silicon wafers which had been implanted with materials that included boron and arsenic. Germanium surfaces were doped using a laser drive-in technique to produce thin contacts for nuclear radiation detectors*. For these and other applications it is necessary that a number of parameters associated with the laser beam be known.

Beam energy

A knowledge of the laser output as a function of input energy, the output reproducibility and the factors affecting this are required. A calorimeter based on the design of Jennings (1966)[27] was built and has been used successfully to measure the Q-switched energy output for a range of input energies. A measure of the width and height of each laser pulse is desirable if the reproducibility of the system is to be monitored. To this end, a system using a fast pin diode has been installed on the optical bench. The laser pulses have been observed on a fast storage oscilloscope and found to have widths typically ∿25 ns.

Beam uniformity

Most of our applications, particularly the production of photovoltaic cells, require that large uniform areas be 'zapped' by the laser. The non-uniformity of the beam spot is a feature of these lasers and, to overcome this, Perspex rods, quartz rods and water-filled glass tubes, all of which use total internal reflections to homogenise the beam, have been used. These have been successful to differing degrees. Irreparable damage occurs to the Perspex after more than a few shots (less than ten). Quartz seems to be more suitable but it is

*E. Lawson, Semiconductor Detector Group, AAEC

27) Jennings, D.A. (1966) - IEEE Trans.Instrum.Meas. IM-15:4

relatively expensive and difficult to shape. (CSIRO is attempting to make two such homogenisers at present). Limited success has been achieved using water-filled glass tubes which are simple to make and inexpensive.

Problems with the Pockel cell have limited the power output from the laser to marginally less than is required for the water-filled homogenisers to operate. These problems should vanish when a new cell is installed.

Vacuum systems

In order to maintain sample purity, it may be necessary to anneal samples under vacuum. A system has been constructed which will allow the laser beam to be introduced through a window to the sample which is under vacuum. The system also allows thin films of a variety of materials to be evaporated or sputtered onto the samples and then be 'zapped' by the laser without removal from the vacuum system.

2.3.4 Solar cell manufacture (A. Rose, M.D. Scott)

A silicon wafer implanted with arsenic was laser annealed and aluminium contacts applied. This cell, although giving an output of only 0.2 V, provided valuable experience in establishing techniques for future cell fabrication.

Reflectivity of semiconductor surfaces

(A. Rose, E. Lawson)

Although the light output from the homogenisers is known, the energy absorbed by the samples under study is not. Surface conditions of these samples vary and hence the reflectivity varies. A calorimeter with a fast response has been built to allow the energy absorbed in samples to be determined. To date, we have successfully measured the reflectivity of a number of samples of germanium and silicon. The technique has been proved to work for relative measurements, but must be improved further if absolute measurements are to be made.

2.3.5 Rutherford backscattering collaborative experiments

(M.D. Scott, M.J. Kenny, M. Farrelly)

A number of Rtherford backscattering and channelling measurements were made in collaboration with other groups from within and from outside the Research Establishment. These are summarised below:

E. Lawson (Semiconductor Detector Group, AAEC)

Backscattering spectra were obtained for elemental analysis of water residues on high purity aluminium. These were needed for dopant profile and

crystal regrowth in pulsed laser melted contacts on germanium, and for inter-diffusion profiles in water-induced corrosion of germanium coated with a thin gold layer.

P. Gillespie (Materials Division)

Measurements were made of the thickness of tungsten films evaporated by electron beam onto a beryllium substrate.

A. Wagh (Bombay Atomic Research Centre)

Spectra were obtained for dopant profile and crystal regrowth in silicon implanted with antimony or indium and annealed by pulsed or continuous wave laser.

B.R. Appleton (Visiting Scientist, ORNL)

The lattice location of nickel impurities in MgO crystals was determined by obtaining channelled spectra along the <100> and <110> axes. Also, in collaboration with CSIRO and ANU, the depth profile was determined for boron in silicon after laser melt in BF_3 gas. This showed a potentially simple method for doping silicon.

A. Brunelli (Telecom and Royal Melbourne Institute of Technology (RMIT)

Channelled spectra were obtained by scanning in 1 mm steps across <100> silicon samples implanted with antimony and annealed by pulsed ruby laser. The spectra showed that crystal structure was restored and that the laser was fully effective over about 7 mm diameter. These samples were used for fabrication of solar cells.

2.3.6 Backscattering facilities

Goniometer and chamber

(M.D. Scott)

A new goniometer and scattering chamber design is being developed in collaboration with RMIT. Two units are to be built, one for use at Lucas Heights and the other for use at RMIT.

Specifications and design were revised following advice and experience gained during the attachment of B.R. Appleton from ORNL. The specifications acopted for the Lucas Heights version include three-axis rotation together with 50 mm of X and Y direction translation in the plane of the target, providing facilities superior to any known Rutherford backscattering goniometer system, commercial or otherwise.

Component selection and layout has been finalised for the first stage of the project - the rotating lid and X-axis tilt assembly. Sketch designs have

been prepared for the remaining angle and X and Y drive. Selection of suitable gears and other components is proceeding.

2.3.7 Beam line vacuum (M.J. Kenny, H.G. Broe)

Rutherford backscattering measurements are very sensitive to impurities introduced onto the sample surface. In particular, carbon contaminants in the vacuum are undesirable. These produce a carbon build-up on the surface at the rate of 60 Å per hour. Accordingly, the entire beam line was overhauled and rebuilt, and a number of minor leaks removed. The pressure in the target chamber dropped by an order of magnitude to 0.1 mPa and carbon build-up was virtually eliminated for beam irradiation for up to 10 μC.

2.3.8 Silicon surface barrier detector calibration (M. Farrelly)

Owing to lack of knowledge of the performance and history of the various surface barrier detectors available, it was decided to record the performance of each detector under standard conditions. A system to do this was set up using a very thin ^{244}Cm α-source* in a small bell jar. Bias voltage up to 100 V was applied while monitoring amplifier output on an oscilloscope. While limiting leakage current to 5×10^{-8} nm at 20°C, bias was optimised by visual minimisation of the broad band noise envelope. Shaping time constants were subsequently selected for optimum resolution. Spectra were stored on floppy disk for future reference.

Approximately half of the sixteen detectors tested achieved the resolution specified by the manufacturers. Poor resolution for the other detectors was probably due to misuse. Generally the resolution at room temperature of Ortec detectors was found to be closer to specifications than that of detectors made by the University of Birmingham.

2.4 Neutron Scattering

In the previous report on neutron scattering (AAEC/PR46, pp.26-29) it was indicated that the AAEC effort in this area had been reduced to one person. The present reporting period has seen the staff in this area increase to three professionals, with no technical support as yet.

An initial task of the reconstituted group was the preparation of documents in support of a 'new policy' proposal to upgrade the neutron diffraction facilities (including the provision of a cold source) at HIFAR. Members of the group made substantial contributions to the Australian Neutron Beam Users' Group Communication to the Australian Science and Technology Council, February 1981.

---

*Courtesy H.A. Wyllie, Radiation Standards Group

Effort is now being applied to the improvement of selected facilities and a number of research projects are under way.

2.4.1 Neutron powder diffraction (C.J. Howard)

The high resolution powder diffractometer, operating now with a single ^{3}He detector behind a high efficiency Soller collimator, records fine diffraction patterns but at very slow rates. The diffractometer has a resolution which, at the moment, is unsurpassed. To improve data acquisition rates, the present collimator and counting system will be replaced by an eight counter array, and it is with this objective that five high efficiency collimators have been purchased. The development will proceed as funds permit.

The diffractometer has been used in a number of studies during the reporting period. Those of interest to AAEC staff include:

- Determination of the oxygen x parameter in rutile by neutron powder methods. A prediction by Bertaut[28] (CNRS, Grenoble) that polarisation effects in rutile would lead to significant differences between neutron and X-ray results for this parameter was tested, and found wanting.
- A neutron powder diffraction study of ZnO, incorporating investigations of preferred orientation.
- Crystal structure of α-UF_5. The fluorine positions differ significantly from those suggested, in earlier X-ray studies.
- A study of the MnPd phase diagram.
- Magnetic structures by neutron scattering. Powder patterns have been recorded from Er_3Al_2 at room temperature and at 4 K. The magnetic lines appearing in the low temperature diffraction pattern have yet to be indexed.

Considerable attention has been paid to the computer programs for 'profile refinement' which are used in analysis of the data. The data from rutile have been regarded as test data for comparing and checking these programs. All existing profile refinement programs include an inadequate account of the 'vertical asymmetry' effects on line profile and efforts to improve this situation are in progress. In connection with the study of α-UF_5, which was prepared in a mixture with U_2F_9, there was a need to implement a version which could analyse the diffraction pattern arising from a mixture of two or more substances. A three-phase version from Bendall[29] (Oxford University) could not be implemented as it

---

[28] Bertaut, E.F.(1978) - J.Phys.(Paris) 39:1331

[29] Bendall, P.J. and Thomas, M.W. (1981) - AERE Report MPD/NBS-165

contained far too many errors. A two-phase version from Wiles and Young[30] (Atlanta) contained a number of serious errors as delivered, but is now close to giving acceptable results.

2.4.2 Neutron inelastic scattering (M.M. Elcombe)

(a) Workshop on triple-axis spectrometer

A very successful workshop giving hands-on experience in operating the triple-axis spectrometer attached to the HIFAR reactor was held on 5-9 April 1981. The object of the workshop was to stimulate greater awareness of the capabilities of the spectrometer for research, the preparations which have to be carried out before experiments are undertaken, and to provide some basic experience in operating the instrument.

Inspiration for the course and a major part of the planning and execution were due to M.C.K. Wiltshire of the Department of Solid State Physics at the Australian National Laboratory. In this he was assisted by M.M. Elcombe and C.J. Howard of the AAEC, T.M. Sabine of the NSWIT and R.L. Davis and F.H. Moore of AINSE. The workshop was organised by AINSE and involved some collaboration with the Australian Neutron Beam Users' Group.

The workshop consisted of six lectures and thirty hours of practical work. It was attended by sixteen scientists from the University of Melbourne, Monash University, the Australian National University, Royal Military College, Duntroon, Commonwealth Scientific and Industrial Research Organisation, Newcastle University, University of Queensland and the New South Wales Institute of Technology.

In the time available, the class split into three groups and operated the instrument in turn, checked the zero calibration, mounted an SrF_2 single crystal and measured the resolution function of the instrument. After these preliminaries, acoustic and optic phonons in the [001], [110] and [111] directions of SrF_2 were measured.

A follow-up survey of participants indicated that the efforts of the organisers were well worthwhile, and further workshops of this type would be both constructive and well-supported.

(b) Realignment of triple-axis spectrometer

From measurements made before and during the workshop it was clear that the spectrometer was not correctly aligned. Mechanical and optical measurements revealed two major problems: (i) the scattering plane of the spectrometer was not horizontal, and (ii) a problem with the measurement of the sample

---

[30] Wiles, D.B. and Young, R.A. (1981) - J.Appl.Cryst. 14:149

scattering angle - as well as a number of minor faults which were easily remedied.

The levels of both the main shield base and the main driving track have been adjusted to give a horizontal scattering plane, the adjustment being carried out by the HIFAR mechanical workshops staff. Despite considerable assistance from Engineering Services and Operations Department (Workshops and Testing and Inspections Sections), the angle measurement problem, in which a zero error of 0.015° is accumulated for every 90° driven up and back, has not yet been solved. Although a 0.015° error in angle would be within the design specifications, the cumulative nature of this error leads to difficulties. To allow continuing use of the spectrometer, frequent checks of the zero on this angle are now being made. Further attempts will be made to eliminate this error, or if that proves impossible, to measure the sample scattering angle in another way.

2.4.3 Small angle scattering (SAS) from biological samples (R.B. Knott)

The AAEC has become directly involved in SAS and molecular biology in recent months. Previous work in this field has been carried out by several university groups under AINSE sponsorship. The basic techniques, particularly in biological membrane research, have now been developed on the modified powder diffractometer on 4H5B. The limitations of the present instrument are now restricting the quality (and quantity) of research that can be undertaken.

Thus far, AAEC involvement has been confined to the design of a new instrument dedicated to molecular biology. The design is the result of collaboration between AAEC and AINSE staff, with the advice of a consultant, Dr. Benno Schoenborn from the Department of Biology, Brookhaven National Laboratory. The new instrument will incorporate the most recent developments in neutron detection, including a 30 cm position sensitive detector which will give an increase in data collection rate by several orders of magnitude in some cases. The wavelength will be increased to $\sim$0.2 nm to improve the angular resolution of the diffraction pattern. Modifications to the neutron shield will reduce the background and improve the quality of the data. The basic design has been finalised and is now being implemented.

3. SEMICONDUCTOR AND RADIATION PHYSICS

3.1 Semiconductor Radiation Detectors

3.1.1 High purity germanium (HPGe) (G.C. Wall, A.J. Tavendale)

It has been decided to terminate this project in the near future following

the impending transfer of a staff member (GCW) and the apparently intractable nature of the problem of consistently producing germanium of acceptable purity for use in radiation detectors. We understand that the major commercial supplier of HPGe in the USA is also having production difficulties at this time and a second company has been unable to produce material of the necessary purity.

We have endeavoured to attack the problem on three fronts. First we examined the chemical thermodynamics of possible reactions between Al, P, Si and O impurities in germanium and attempted to interpret the experimental measurements of many crystals in terms of these. Second, additional experiments were made in which germanium bars highly doped with these elements were normally frozen. Analysis of this material by spark source mass spectrometry is to be made in an effort to detect possible interactions, especially between Al and P.

Third, a detailed investigation of the multiple crystal growth process, which is used by the General Electric Company to produce high purity germanium commercially, was carried out during this period. This process depends on the fact that normally segregating impurities would concentrate towards the 'tail' end of the crystal. Thus, if the top halves of crystals are combined and used to grow second generation crystals, a more pure product should be obtained. In principle, this process could be repeated a sufficient number of times to give the desired level of less than 5×10^{10} net electrically active impurity atoms per cm^3.

In our investigation, eight first generation crystals were grown from charges cut from two bars of Eagle Picher zone-refined intrinsic germanium. The tops of these crystals were used to produce four second generation crystals and so on, finally yielding one fourth generation crystal. In addition, the lower halves of the crystals were combined and regrown in a similar way. In all, 32 crystals were produced in the experiment.

The results are still being analysed, but so far the following points have been established:

1. The impurity profiles of the first generation crystals could be correlated with the positions in the zone-refined bars of the charges from which the crystals were grown. This suggests that any contamination during crystal production was not dominant in determining impurity content.
2. The net acceptor level of the fourth generation 'pure' crystal was 5×10^{11} atoms cm^{-3} (i.e. a factor of 10 too high). The impurity profile of this crystal was almost identical with that of the best of the first generation crystals. It was also very similar to the profiles of the two third generation crystals.

3. There was a close balance of acceptor and donor concentrations in the third and fourth generation crystals. The process appears to improve this balance rather than to reduce the actual impurity concentrations.
4. The later generations produced from the 'dirty' ends of the crystals became progressively more n-type, but a corresponding decrease in donor levels in the 'clean' crystals was not observed. This cannot be due to donor contamination during processing in view of the close donor-acceptor balance observed in the 'clean' crystals.
5. The model proposed by R.N. Hall[1)] of General Electric to explain the shape of the impurity profile does not fit the results.
6. A qualitative explanation of the results is as follows:
   (a) The initial charges contain an electrically inactive donor-acceptor compound plus an excess of free donor or acceptor.
   (b) Regrowth of the tops of crystals eliminates the excess donor or acceptor and gives crystals which have a close balance of donor and acceptor from the dissociation of the compound.
   (c) An addition of oxygen to the melt from the quartz crucible occurs on each regrowth.
   (d) Oxygen has the double effect of suppressing free acceptors and releasing free donors from the donor-acceptor compound.
   (e) Oxygen segregates towards the tail ends of the crystals during growth. This results in later generation crystals from the tops reaching a constant oxygen level, while crystals from the bottoms become increasingly oxygen-rich in later generations. As a result of this, the crystals from the tops reach a stable net impurity profile, while the crystals from the bottoms become progressively more n-type because of donors released by the increasing oxygen concentration.

It seems likely that this process can work only if the concentration of donor-acceptor compound in the initial zone-refined charge material is sufficiently low, or if a critical amount of another, more effective, complexing element (perhaps silicon) is present.

---

1) Hall, R.N. and Soltys T.J. (1971) - I.E.E.E. Vol. NS-18, (1) : 160

Other work during this period included the growth of numerous crystals under modified preparation and etching conditions to look for evidence of contamination during processing. No such evidence was found. In addition our work on computer modelling of the zone-refining process was continued. Use was made of the CSIRONET THERMODATA system to determine the stability of possible donor-acceptor compounds.

3.2 Nuclear Radiation Detectors (A.J. Tavendale, E.M. Lawson, D. Alexiev, S. Pearton*, A. Williams, P. Lee)

3.2.1 Construction and maintenance of semiconductor detectors

(a) Silicon X-ray fluorescence detectors for mineral analysis

The development of a bench top unit and a slurry immersion silicon X-ray detector probe is progressing satisfactorily. This work is being carried out in association with the Radioisotope Applications Research Section and is funded by the Australian Mineral Industries Research Association (AMIRA).

Several sections of 'Topsil' silicon have been lithium drifted and test X-ray detectors constructed from this material which appears to drift normally. Preliminary measurements on the first detector indicate that acceptable leakage currents should be obtained at an operating temperature of -90° C, the temperature at which the Peltier-cooled 'front-end' is designed to operate. Microphonic effects appear to be minimal in the newly designed detector mount.

(b) Large coaxial Ge(Li) detector construction

The construction of a large volume (~80 cm^3) coaxial, lithium drifted germanium detector was begun during the period. This detector will be employed as an emergency replacement device. At the present time, the Radiation Detector Group has no functional standby Ge(Li) detector for such situations as arise during detector maintenance.

(c) Detector Maintenance

During the period, one large coaxial Ge(Li) γ-ray detector and one silicon X-ray detector required reprocessing due to failure to maintain liquid nitrogen coolant supplies by the users.

3.2.2 Contacts on semiconductors

(a) Motion of Ge through thin Au layers at low temperatures

We have observed a very obvious change in appearance in thin ($\lesssim$20 nm) layers

*AINSE student

overlying Ge substrates when stored for long periods (~3 years) at room temperature in a humid atmosphere. When examined by scanning electron microscopy, crystallites were observed to have formed on the Au; later this was identified as GeO_2 using X-ray diffraction. It appears that Ge has mixed with, and moved through, the Au allowing oxide production on the surface. This process is occurring well below the Au-Ge eutectic temperature of 356° C. Such observations suggest that the room ambient storage of Ge nuclear radiation detectors with Au may prove deleterious.

To study the process, we have subjected Au coated Ge samples to a variety of treatments, all of which were carried out at 100° C, in order to increase the rate of oxide production. Changes in ambient atmosphere, time, crystal orientation, and Ge surface prior to Au evaporation, were studied using RBS. We found that a high water vapour content increases the oxide production rate whereas an oxide finish on the original Ge surface tends to inhibit the process. Orientation effects have been seen. It is intended to make similar studies of Pd on Ge - since Pd is also commonly used as a detector contact.

(b) Laser doping of semiconductors

These studies were continued. In particular, In and Sb contacts to Ge were investigated more thoroughly. Parameters such as solubility, Ψ min, distribution FWHM and substitutional fraction were obtained using RBS. The substitutional solubility was also determined electrically by Van der Pauw Hall measurements at 77 K. Reasonable agreement was found. The substitutional solubilities measured were well above the maximum equilibrium values. (A paper describing this work has been submitted to the Journal of Applied Physics.)

(c) Nitrogen in Germanium

Studies of the electrical activity of nitrogen implanted in germanium at 90 keV (RMIT) and 1 MeV (AAEC Van de Graaff accelerator) were continued. Donor activity was detected following thermal annealing over a narrow temperature range (500-600° C). Laser melt-annealed (Q-switched ruby laser) samples also showed donor activity but again only after additional thermal annealing. In order to make use of the deep level transient spectroscopy (DLTS) technique to help clarify the nature of the apparent nitrogen donor in germanium, further implants into more highly doped base material are required.

3.2.3 Deep level transient spectroscopy studies of semiconductors

(a) Radiation damage in Ge

Experiments on a wide range of material identified oxygen-vacancy complexes

as the cause of the common E_v to 0.23 eV and E to 0.38 eV acceptor levels in γ-irradiated Ge pulled from silica crucibles in an H_2 atmosphere. Subjecting such crystals to a heating cycle before irradiation reduced the amount of free oxygen available to participate in formation of the levels, leading to a method for hardening silica grown crystals to γ-radiation damage. Experiments were performed on the stability of γ-induced damage centres to thermal annealing, high electric and magnetic fields, and stress induced in the crystal.

(b) Laser melted contacts

Successful laser doped Li contacts were fabricated on approximately 20 Ge and 8 Si radiation detectors. Excess laser power and resulting damage in the laser melted region was identified by I-V and DLTS measurements as being the cause of the poor detection responses of some diodes. The Li acts to passivate some of the damage enabling a higher yield of detectors than with other dopants.

(c) Deep metal centres in Ge

Deliberate doping of Ge was performed (by diffusion) using the following elements: Au, Ag, Ni, Pt, Pd, Cd, Te, Co, Cr, Fe, Mn, Mg, Ba, Ti, Zr, Si, Sn, Pb, S, Se, Nd, Gd, Tb, Ho, Er, Zn, Mo, Bi and Tm. The resulting impurity levels were recorded by DLTS, producing reference fingerprints for these elements. Many of the elements have similar capture and emission properties within the Ge lattice, supporting the view that they form defect complexes with other impurities and lattice defects already present.

(d) Hydrogen passivation of defects

Troublesome copper-related defects in Ge can be passivated by inserting the Ge sample in an atomic hydrogen plasma. The H acts to neutralise defective bonds related to impurities, and the method may have application to some Ge devices. A 3-hour plasma exposure at 300° C passivates 90% of the copper centres at a depth of ~100 μm. A deep donor level in GaAs was also passivated by this means. The diffusion of hydrogen is much slower in GaAs, however, a 3-hour plasma exposure at 250° C neutralises levels to a depth of ~1 μm.

3.2.4 Instrumentation: development, construction, maintenance and purchases

(a) Sputtering system

The design and construction of a turbomolecular pumped (120 L s^{-1}) sputtering system was completed. This system can be used for d.c. sputtering of thin films for contacting semiconductor detectors. Induction coupled RF (27 MHz)

power is available for generation of gas glow discharges (for example, when hydrogenating semiconductors). The facility is a considerable advance on the crude vacuum station used for sputtering and can provide an essentially oil-free environment.

(b) Single ion pulse detection system for the spark source mass spectrometer

The final assembly and testing of this system has been made. A modification was made to enable the ADC pulse train from the Nuclear Data 181-F pulse height analyser to be scaled into the associated PDP11 computer. This facility permitted weighting of the input signal in terms of the amplitude of the spectrometer secondary ion multiplier detector pulse. Several test samples were sparked and spectra recorded.

Although the detection system functioned, as predicted, detection limits were higher than expected and variable due to severe background electrical noise distrubances. These were traced to burst noise from a precipitor in a nearby exhaust stack and earth loop noise at the input of the low noise preamplifier mainly associated with the spectrometer RF spark generator. Full benefit from the detection system will only be obtained providing the secondary ion multiplier and preamplifier combination can be electrically isolated from the mainframe of the spectrometer.

(c) Search for phosphorus contamination in the Millipore water system,

Evidence for P was sought and found in water from the Millipore 'Super-Q' high purity water system. Samples of water were evaporated from drops placed on a variety of substrates and the residue then examined using RBS. Glassy carbon substrates were found unsuitable because of high, and variable, impurity concentrations. Single crystal, <111> oriented, Si substrates were also tried and some evidence for P was found. Although the Si substrates were channelled to reduce the background, the P and Si were not well enough resolved to provide conclusive proof. High purity Al substrates were used and provided definite evidence for P in the water. Although these substrates could not be channelled, the separation between P and Al was quite adequate.

(d) Equipment purchase

The Canberra Series 80 multichannel analyser and Teletype Model 43 printer were received and are now operational but not without problems. The analyser was delivered in a damaged state.

3.2.5 Requests for assistance

During the period, the Radiation Detector Group received two visiting scientists interested in the technical aspects of detector manufacture and nine enquiries were made requesting advice on detector usage and specifications for commercial purchases.

3.3 Radiation Standards Group (G.C. Lowenthal, H.A. Wyllie, V. Page)

3.3.1 Radioactivity

(a) International involvements

The Group Leader represented the AAEC at the Section II Meeting of the Consultative Committee on the Measurement of Ionising Radiation which took place at the International Bureau of Weights and Measures, Paris, from 3rd to 5th May, 1981, and subsequently at the Scientific Meeting of the International Committee on Radionuclide Metrology (ICRM) held in Warsaw, Poland, from 11th to 15th May, 1981.

The Section II Meeting discussed (among others) results of an international comparison of ^{55}Fe conducted during 1979 and also results obtained at Lucas Heights by means of a new method employing very thin sources (see below). It was decided to set up a Working Group on Thin Sources and to invite the AAEC to act as convenor.

At the ICRM meeting, the Standards Group presented two papers; one on a chemical method for making ultra-thin alpha and electron sources, a method developed by H.A. Wyllie, and the second paper on procedures for the measurement of γ-peak areas (see below).

3.3.2 New activity standardisations and other developments

(a) ^{55}Fe

The new method developed to measure the activity of ^{55}Fe was brought to a satisfactory conclusion and a paper on this work has been submitted for publication. Iron 55 is of great interest for the intensity calibration of low energy photon detectors but results obtained during a 1979 international intercomparison ranged over nearly 7.0%. The AAEC result supports other well-based results near the upper end of the 7% range. It was obtained using ^{51}Cr and ^{54}Mn as tracers but it appears that the two-gas method employed for these measurements could permit a self-tracing procedure. The activity of ^{109}Cd could probably be measured in a similar way. This nuclide would be very useful for the calibration of Ge(Li) detectors if its activity could be measured more accurately than at present. Preparations are being made to apply our new method to ^{109}Cd

standardisations which will be of particular interest since the BIPM plans a limited international comparison for this nuclide.

(b) The electrical resistance of thin sources

Methods used here and overseas to reduce the 4π counting efficiencies of radioactive sources, e.g. to obtain data for efficiency extrapolations, led also to increases in source resistance: measured values were 10^5 to 10^7 ohm instead of the preferred range 10^2 to 10^3 ohm. To avoid this increase, a method was developed by H.A. Wyllie in which silver acetate is electrosprayed over the area of the source and is subsequently reduced to silver. As little as 1-2 $\mu g\ cm^{-2}$ of silver is sufficient to keep the resistance of sources to around 100 ohm but 100 $\mu g\ cm^{-2}$ or more can be applied easily, without damage to the source or its support. Although high resistance sources have been counted with satisfactory results, the ability to ensure in a relatively simple way that source resistances seen by the electric field inside the 4π counter are always adequately low, is a valuable gain.

(c) γ-spectrometry

Limitations on available instrumentation make it desirable to analyse γ-spectra into 1.0 to 1.6 keV/channel intervals but this increases the risk of errors in the measurement of peak areas. It was necessary, therefore, to devise procedures which could be relied upon to keep uncertainties within 1.0%. Two methods were developed and tested with satisfactory results. The method developed by V. Page was adapted for a T159 programmable hand calculator, bringing gains in time and reliability.

(d) ^{176m}Lu for cosmochronology

This is a Physics Division project (B.J. Allen) reported on in earlier progress reports. The experiments were then made with Lu_2O_3 powder. They have been repeated with a lutetium metal foil to check on possible effects due to oxygen but results agreed within the estimated uncertainties. The work has now been accepted for publication, as was a paper on the remeasurement of the decay scheme data of ^{176m} Lu.

The latter paper was written at the Research Establishment but described work performed by the Group Leader as visiting scientist at the Laboratoire de Metrologie des Rayonnements Ionisants, Saclay, France.

3.3.3 Services

A revised pamphlet to inform on the range of sources with standardised

disintegration rates, now available from the AAEC, is still waiting to be printed.

Services were supplied within and outside the Research Establishment at an average rate of five per month involving 20 different radionuclides.

3.4 Absorbed Dose (D.F. Urquhart, E.P. Johnson)

3.4.1 Primary standard of absorbed dose

The installation of a new thermistor and 3 spare thermistors in the absorber of the calorimeter was completed. The calorimeter was re-assembled and a trial dose measurement made. The result agreed with dose measurements made before the failure of the thermistor. The additional leads from the three spare thermistors were found to produce a noticeable reduction in the thermal isolation of the absorber. It was decided to remove the spare thermistors and the calorimeter was therefore dismantled again. The modifications which have been made to the calorimeter now make it possible to replace a faulty absorber thermistor in a few days, so in situ spares are not essential.

3.4.2 Working standards of absorbed dose

A report summarising work on the calibration of the working standards of absorbed dose to water and carbon, was sent to the Chairman of an international working party, set up by Section I of CCEMRI,* to study the problem of the transfer of dose from a carbon calorimeter to water. This report was subsequently tabled at the June 1981 meeting of CCEMRI in Paris and given the number CCEMRI(I)/81-34. The proceedings of this meeting will be published.

3.4.3 International comparison of absorbed dose measurements

In November 1980, the International Atomic Energy Agency (IAEA) conducted an international thermoluminescence dosimetry (TLD) postal intercomparison of absorbed dose to water measurements. This gave the AAEC the first opportunity of comparing its standards of measurement with those of other countries. Measurements from 22 laboratories were compared with measurements made at IAEA in Vienna. The AAEC was the only laboratory to use measurements based on calorimetry; all the others used conventional ion chamber methods. For this comparison, the detectable systematic uncertainty (95% confidence level) was ±2%. The AAEC results differed from those of the IAEA by +1.2%. The mean for all the other 22 laboratories differed from the IAEA by +1.0%.

---

*Consultative Committee for Standards of Measurement of Ionising Radiation, Section I covers X- and γ-rays and electrons.

3.4.4 Staff

Progress in the radiation standards work is now severely restricted by inadequate staffing. For the period under review, W. Badger was transferred full-time to the Instrument Development Group, and P. Johnson receives regular study-leave for a part-time degree course.

3.5 Special Studies Group (A.W. Pryor, J.E. Eberhardt)

3.5.1 Laser isotope separation

Some experiments on this project continued until February 1981. The object of experiments during these last few months was to round out data preparatory to publication. Systematic observations of the multiphoton decomposition of ethyl acetate in a wide range of both gases were completed. Decomposition of uranyl compounds was observed at pressures up to 60 Pa, a regime of little promise as regards isotope separation but of some theoretical interest.

In February 1981 much of our major equipment, in particular the continuous CO_2 laser, was transferred to Chemical Technology Division and we ceased experimentation in the multiphoton dissociation field.

A considerable effort has been given to the theoretical analysis of multiphoton dissociation. A computer program of "energy-grained master equations" has been written and employed in the analysis of the ethyl acetate data. Having established its validity, the same technique will be used for the analysis of data acquired for the uranyl compounds in the period 1978-1980.

3.5.2 Hydrogen fluoride monitor

After some consideration of various possibilities in the general area of pollution monitoring, we have proposed a method of measuring the atmospheric concentration of HF in the pot-rooms of aluminium smelters. This is a problem of pressing industrial concern to which we can offer an elegant solution. We have noted a fortuitous coincidence between the 1R5 absorption line of HF, at 2.39 μm, and the $3p_4$-$2s_2$ line obtainable from a He-Ne laser. In laboratory trials, we have studied the HF absorption of this laser line, shown that the He-Ne laser can also provide a nearby line ($3p_2$-$2s_2$) to act as reference, and shown that there is little interference from H_2O, CO_2 or CO. A provisional patent application has been filed and we have met with representatives of the aluminium companies to enlist their support for the development of an instrument.

4. ELECTRONIC SYSTEMS

4.1 Instrument Maintenance (M. Dilli, G. Carter, E. Arady, A. Godwin, R. Klausch, E. Mutch, D. Papac, R. Phillips, W. Swanston)

During this period 528 electronic instruments were serviced. A further 396 new instruments were inspected and/or tested for acceptability.

Two Malaysian trainees from Puspati were attached to the group to gain maintenance experience.

4.2 Project Instrumentation (R.M. Hicks, D.H. Rice, R.J. Sanders, A. Andrews)

4.2.1 HIFAR emergency core cooling systems (ECCS)

The group has undertaken the design, fabrication, installation and commissioning of instrumentation and control equipment which will automatically initiate operation of the emergency core cooling system in the event of a loss of coolant accident. Much of the detailed design is now complete and the second stage submission is being prepared for the Licensing and Regulatory Bureau. (Being part of a protective barrier, this system is required to comply with internationally accepted safety codes.)

4.2.2 Hippocrene and Freon rigs

The installation and commissioning of a microprocessor-based data acquisition system has been successfully completed and the commissioning of the automatic flow, temperature and level controllers is continuing.

4.2.3 HIFAR - neutron flux channels

Acceptance testing was suspended owing to the failure of the equipment to comply with design specifications. The units were returned to the supplier for modifications.

4.3 Instrument Design (H.J. Fraser, G.C. Watt, A.N. Bransgrove, G.A. Phillips)

4.3.1 Centrifuge enrichment power supplies

A 3 kW series resonant load commutated circuit has been designed and parts obtained for its development. Some of the circuitry is not yet finalised as this will depend upon interfacing the supply with a bank of motors. There has been limited effort in this project owing to staff shortages.

4.3.2 Radiation monitoring

(a) A new circuit (type 650) was designed to replace the type 450 area gamma monitor. Type 650 is the preferred development of the 627/628 designs. It is now fully developed and ten have been wired under an external wiring contract. The type 650 has a three decade log scale, whereas the type 450 has two switched ranges. The new design eliminates possible errors in scale reading.

(b) No progress has been made on the type γ-β survey meter owing to staff shortages.

(c) Four sets of nuclear ship monitors have been completed. One of these is installed at Stirling Naval Base, W.A. Radio frequency interference testing was carried out at Garden Island naval facility and the equipment performed without malfunction.

4.3.3 Other instruments designed and/or manufactured

- Extension rig 182 strain measuring circuit.
- Modification to change range of 20 channel temperature scanner and to install better amplifiers.
- Three-current integrators (type 619) for tritium electrolysis equipment.
- Five electrometers, type 612.
- Linear ratemeter, type 634.
- Additional electronics for 1 MeV accelerator beam control and light measurements.
- One variable frequency power supply controller.
- An investigation was done on microprocessor data logging equipment for Physics of Environment Section.
- Two pulsed optoelectronic low noise preamplifiers, type 654.

4.4 Systems Analysis

4.4.1 HIFAR simulator (N.R. Clark)

A major task recently completed was the transfer of the HIFAR simulator computational procedures from an analogue computer to the hybrid computer system. (This simulator is maintained so that reactor operators may be familiarised with reactor procedures without actually using the reactor.) The transfer was undertaken because the 231R analogue computer is now obsolete.

As the hybrid computer offers both digital and analogue computation, either separately or interactively, the reactor model was completely redesigned

to make best use of this versatile machine. The analogue portion of the machine is reserved for the neutron kinetics calculations, where high speed and accuracy are important, while the solution of the heat transfer through the reactor cooling circuits and all safety-related logical operations are carried out by a monitor program in the hybrid's digital computer. (The logice used to be implemented by electronic hardware built into the simulator console.) Both the monitor program and a high speed data interface between the digital computer and the operator's console were designed and built by the group. The opportunity was taken to include some modifications to the heat transfer terms in the model equations so as to give a better match to recent measurements made on HIFAR's cooling towers. The result is a simulator with considerably more flexibility, greater ease and speed in setting up, and which is less subject to electrical interference than the original machine.

4.4.2 Dynamic analysis (C.P. Gilbert, P.C. Miskelly)

Considerable effort has been expended in the application of frequency response analysis to problems arising within the Centrifuge Enrichment Project Division.

4.4.3 Digital systems (P.J. Ellis, D.J. Reid, C.G. Laman, N.M. Hudson)

(a) SMUT

A new video processor-based SMUT control unit has been developed and undergone operational tests. This unit was constructed using one printed circuit board which eliminates the back-plane wiring required for the older units. The new unit also has the added advantage that the 8085 microprocessor and its associated eraseable, programmable, read only memory can be reprogrammed if changes in operation have to be made. The current operating program is capable of buffering both input and output characters, varying responses according to syntax signals sent from the controlling NOVA computer and adjusting baud rate on 'power up' to match six standard baud rates. Thirty of these units are being manufactured by AAEC staff and an outside contract for another twenty is to be commenced as soon as possible.

(b) Dataway

Owing to several faults on the PDP9L computer which controls the main databank to the IBM3031, it has been necessary to develop an alternative pathway to handle the traffic during any lengthy downtime of the existing system, as well as to augment the overall data handling capability. The main components

of this system are:

1. A multiprocessor 8086 based computer system.
2. An interface between the IBM3031 channel and the multiprocessor bus.
3. The interface between the Dataway and the multiprocessor bus.

The multiprocessor is a commercial item which has been in operation for some time and consists of three Intel 86/12 single board computers. The IBM channel to the Intel multibus interface has been developed and is undergoing operational tests. This interface is capable of handling any of the current IBM channel conventions and can be easily modified, if necessary, to handle future changes. The Dataway to multibus interface is being developed and individual units are being tested.

5. FUSION PHYSICS

5.1 Data Library (B.E. Clancy, J.L. Cook, E.K. Rose)

Replacement of impurity data by the data of Post et al.[1] for power rate coefficients

These data were originally reported in the form of polynomials in logarithm electron temperatures with different polynomials covering different temperature ranges. The polynomial values were generated at a grid of temperature values, and discontinuities were observed at the temperature values corresponding to the points at which two different polynomial functions could apply. These discontinuities were removed by 'eyeball' smoothing after removal of the bremsstrahlung contribution.

5.2 SCORCH Code Development (B.E. Clancy, J.L. Cook)

A number of minor modifications to the SCORCH code reported previously were made during the period. The most significant change was to include the possibility of time variation of the toroidal current and consequently the poloidal magnetic field. This gives the code the possibility of simulating the evolution of ion and electron temperatures during the start-up phase of experimental plasma devices.

The code was used to simulate the start-up stage of the University of Sydney TORTUS tokamak machine at present being commissioned.

---

[1] Post, D.E., Jensen, R.V., Tartar, C.B., Grassberger, W.H. and Lokke, W.A. (1977) - At. Data Nucl. Data Tables 20:5

5.3 Australian National University

5.3.1 Soft X-ray measurements on the LT-4 tokamak

(G.R. Hogg, W.K. Bertram)

New plasma position feedback control systems have been installed on the LT-4 tokamak and it is now possible to produce plasmas with a discharge length of ~120 ms and which are stable to better than ±1 mm in both the radial and vertical positions. Present plasma operating conditions are with a toroidal magnetic field of 2.5 T and plasma discharge current of 60 kA. Thomson scattering measurements indicate an electron temperature in the range 300-400 eV and an electron density of up to 4×10^{19} m^3 has been obtained through the use of a preprogrammed gas puffing system. Electron cyclotron radiation measurements indicate that the plasma is essentially free of runaway electrons.

The seven-channel diode array has been commissioned on LT-4 and measurements of the soft X-ray fluctuations of the plasma have been obtained. These exhibited the usual saw-tooth relaxations associated with minor electron temperature fluctuations and magneto-hydrodynamic (MHD) instabilities associated with the q=1 and 2 surfaces. It is planned to unfold the raw data and evaluate the radial and temporal evolution of MHD modes (magnetic islands) within the plasma.

The energy spectrum of the plasma X-ray emission has been measured with a liquid nitrogen cooled silicon detector. The plasma electron temperature derived from this measurement is in general agreement with the Thomson scattering result but further refinement of the system is required. This involves modification to the pulse pile-up detection circuitry to improve the energy resolution and to the radiation shielding of the detector.

5.3.2 Calculation of plasma transport properties for LT-4

(W.K. Bertram)

Since the recent successful operation of the LT-4 tokamak, calculations of the plasma transport were performed using the computer code HERMES. These calculations simulated operating conditions similar to those of the LT-4 plasma under test. Although no detailed experimental measurements for the LT-4 plasma are yet available, the calculated transport properties were quite consistent with those observed in the test plasma.

To simplify the analysis of plasma transport coefficients, we are investigating a method for deducing these parameters more directly from experimental data. This method is based on the assumption that during the time

that measurements on the plasma are made, it is in a transport equilibrium.

Another task undertaken was the modification of the Princeton equilibrium and stability code, PEST, to produce a version which would allow us to run the equilibrium part of the code on the DEC10 computer. After some difficulties, mainly with the coding for the graphical output, this was recently completed and our simplified version of PEST runs satisfactorily on the DEC10.

5.4 Flinders University of South Australia (J. Tendys, G. Durance)

The studies of non-linear excitation of magneto-acoustic oscillations by means of an oscillating axial current have been completed. Experiments at nine different frequencies were performed in an argon afterglow plasma in FUZA-2. The results were found to be in excellent qualitative agreement with a perturbation analysis. An improvement in quantitative agreement was obtained by the incorporation of an anisotropic plasma conductivity into the analysis. The use of these magneto-acoustic oscillations as a plasma diagnostic technique for the determination of electron number density was investigated, and good agreement with laser interferometric density measurements was found.

The instability measurements have also been completed and analysed. From the computer code analyses, it was found that the measured equilibria were unstable to m = 1 instabilities with growth times ranging from 0.5 to 1.3 μs and with wavelengths of 0.09 to 0.20 m. The resistive code gave predicted growth times and wavelengths somewhat longer than the ideal MHD code. The experimentally measured values for the growth times agreed well with the predictions of the resistive code for well-compressed columns. The more diffuse columns had growth times up to twice as long as the predicted values. In most cases the measured wavelengths were in reasonable agreement with the calculated ones using the resistive code. The above work has been reported by J. Tendys FUPH-R-174 [1981]) and S. Huxford (M.Sc. Thesis, Flinders University, S.A. [1981]).

The above studies concluded the investigations on FUZA-2. Research effort is now concentrated on the production of plasma currents by rotating magnetic fields and, in particular, on the application of this technique to the production of a compact torus configuration (the so-called rotamak). Preliminary studies of the rotamak concept have been published by Hugrass[2)].

This year the effects of vessel size, gas type and filling-pressure,

---

2) Hugrass, W.N., Jones, I.R., McKenna, K.F., Phillips, M.G.R., Storer, R.G. and Tuczek H. (1980) - Phys. Rev. Lett. 44:1676 (1980).

and bias field strength were investigated. These were essentially exploratory experiments and only the toroidal current was monitored. This current typically exhibited the same general form as that observed in the earlier experiments of Hugrass et al.[2] i.e. a peaked formation phase followed by an equilibrium plateau. In the present experiments, however, the duration of the currents, and in particular the plateaux, were substantially longer (up to $\sim$ 50 μs) corresponding to the wavetrain duration from the new line generators used to produce the rotating field. The experimental results show excellent agreement with computer calculations using the equilibrium code ROTA (adapted from the PEST code).

Under certain conditions, a second smaller current plateau was observed, and has been interpreted in terms of a mirror-field configuration. This suggests that the rotating field technique may have applications to the 'end-plugging' of conventional mirror-fields.

Overall the results appeared very encouraging. In particular there was no evidence of instabilities. And here it should be noted that these experiments were performed without the application of steady toroidal fields and without the use of conducting shells. Under such conditions a conventional compact torus is predicted by MHD theory to be highly unstable. More detailed measurements are now required to confirm the interpretations placed on the experimental results.

To complement these studies, a 6 kW radiofrequency-generator is being prepared. Although the low output power is a limitation, the long ($\sim$ 10 ms) wavetrains available should enable such long-term effects as ion spin-up to be studied. To date the main problem has been the design and construction of a unit to appropriately divide and phase-shift the generator output.

These studies have been carried out in association with university staff and research students.

5.5 Sydney University (I.J. Donnelly)

5.5.1 MHD surface waves

A constant density plasma column surrounded by a plasma of lower density and then a conducting boundary presents a convenient model for the estimation of some properties of MHD waves in a tokamak. For frequencies well below the ion cyclotron frequency, this model has been used to analyse the wave behaviour as a function of the plasma density distribution and the wavenumber. The lowest frequency magneto-acoustic wave which can exist is, under most circumstances, a

surface wave in which the wave fields decrease with distance from the plasma-plasma interface. Higher frequency wave modes are body waves with spatially oscillating fields in the denser plasma.

The surface waves have been analysed in detail as they are of interest for coupling the radiofrequency energy to the plasma. Their properties are indicated by the following simple analysis of the plane interface between a plasma of constant density ρ and a vacuum. A constant magnetic field $B\hat{z}$ is present and $\hat{x}$ is normal to the interface. Wave perturbations of the form

$$\underset{\sim}{b}(\underset{\sim}{r}) = \underset{\sim}{b}(x) \exp i(k_y y + k_z z - \omega t)$$

are assumed and the MHD equations are solved to give the dispersion relation

$$\omega_s^2 = \frac{2k_y^2 + k_z^2}{k_y^2 + k_z^2} v_A^2 k_z^2$$

where

$$v_A^2 = B^2/\mu_o \rho$$

The field components b_x, b_z and v_x are continuous at the interface while b_y and v_y are discontinuous. This indicates that resistive and viscous damping are important in the surface region. The relative magnitudes of the wave fields are determined mainly by the value of k_y and k_z, with the magnetic field compression, b_z/b, reaching a maximum in the plasma when $k_y \simeq k_z$, and falling to zero for small and large k_y. Therefore, at least in the denser plasma, the surface wave has properties similar to those of an Alfvén shear wave unless $k_y \simeq k_z$, in which case it is similar to a compressive wave.

6. PUBLICATIONS AND TALKS

6.1 Journal Papers

Allen, B.J., Cohen, D.D. and Company, F.Z. (1980) - Radiative widths of neutron scattering resonances. J. Phys. G. 6:1173.

Allen, B.J., Lowenthal, G.C. and de Laeter, J.R. (1981) - s-process branch at ^{176}Lu. J. Phys. : Nucl. Phys. (in press).

Bird, J.R., Rose, A. and Wilkins, R.W.T. (1981) - Porton decoration of halite crystals. Aust. J. Phys. 34.

Clayton, E., Cohen, D.D. and Duerden, P. (1981) - Thick target PIXE analysis and yield curve calculations. Nucl. Instr. and Meth. 180:541.

Cohen, D.D., Clayton, E. and Ainsworth, T. (1981) - Preliminary investigations into trace element concentration in human teeth. Nucl. Instr. and Meth. 188:203.

Cohen, D.D. (1981) - HIXE A comparison of experimental ionisation subshell cross sections with PWBA, PWBAR and CPSSR Theories. Nucl. Instr. and Meth. 191:551. Also 5th Int. Conf. Ion Beam Anal., Sydney.

Cohen, D.D. (1981) - L subshell ionisation cross section for Au and Pb by He^+ bombardment. J. Phys. B: Atom. Mol. Phys. 14:2037.

Golja, B., Nassibian, A.G. and Cohen, D.D. (1981) - Ion implant gettering of generation impurities in silicon investigated using PIXE and RBS. Nucl. Instr. and Meth. 191:63. Also 5th Int. Conf. Ion Beam Anal., Sydney.

Golja, B., Nassibian, A.G. and Cohen, D.D. (1981) - PIXE studies of generation impurities in silicon. IEEE Proc. 128:68.

Kenny, M.J. (1981) - Thick target gamma ray yields from fluorine. Aust. J. Phys. 34:35.

Lawson, E.M. (1981) - Laser doping - a method for producing thin contacts on semiconductor nuclear radiation detectors. Nucl. Instr. and Methods, 180:651.

Lowenthal, G.C. (1980) - Standards of radioactivity - An AAEC contribution to the science of measurement. Atom. En. Aust. 23(3):22.

Lowenthal, G.C., Morel, J., Bac, C., Lagoutin, F. and Vatin, R. (1981) ^{176m}Lu: A remeasurement of its half-life and of the energies and intensities of photon emissions following its decay. J. Phys. : Nucl. Phys. (in press).

Lowenthal, G.C., Wyllie, H.A. and Page, V. (1981) - A method for measuring the activity of ^{55}Fe using a 4π proportional counter. Int. J. Appl. Radiat. Isotopes (in press).

Musgrove, A.R. de L., Boldeman, J.W., Cook, J.L., Lang, D.W., Rose, E.K., Walsh, R.L., Caruana, J. and Mathur, J.N. (1981) - Fragment angular distributions from neutron-induced fission of ^{233}U and ^{235}U. J. Phys. G : Nucl. Phys. 7:549.

Pearton, S.J. (1981) - Magnetic field dependence of defect state in GaAs. Phys. Stat. Sol. (b) 105:K19.

Pearton, S.J. and Williams, A.A. - Ultra-thin laser aided doped Li contacts on HPGe nuclear radiation detectors. Nucl. Instr. and Meth. (in press).

Pearton, S.J. - The use of laser aided doped Li contacts on semiconductor nuclear radiation detectors. Nucl. Instr. and Meth. (in press).

Raman, S., Slaughter, G.G., Wells, J.C. Jr., and Allen, B.J. (1980) - Valence neutron capture gamma ray spectrum in ^{54}Fe. Phys. Rev. 22:328.

Sabine, T.M. and Howard, C.J. (1981) - Determination of the oxygen parameter in rutile by neutron powder methods. Acta Crystal. B (in press).

Silawatshananai, C., Anderson, F.S.B., Brennan, M.H., Durance, G., Jones, I.R., Murray, E.L. and Tendys, J. (1980) - The effects of preionisation level on a 'stabilised' Z-pinch. Aust. J. Phys. 33:1001.

Wilkins, R.W.T., Bird, J.R. and Ewald, A.H. (1981) - Observations on deformation microstructures and fluid inclusions in proton-irradiated halite. Neues Jahrbuch für Mineralogie Monatshefte.

Wilson, D.J. and Bentley, K.W. (1981) - The measurement of the range of fission fragments in tissue and the plutonium burden of mouse liver by neutron induced autoradiography. J. Rad. Eff. 56:187.

Wyllie, H.A. and Lowenthal, G.C. (1981) - An electrospraying technique for coating radioactive sources with silver. Int. J. Appl. Radiat. Isotopes (in press).

6.2 External Reports

Clancy, B.E., Cook, J.L. and Rose, E.K. (1981) - ADL-1: An atomic data library for use in computing the behaviour of plasma devices including fusion reactors. AAEC/E515.

Walsh, R.L. and Senior, I.F. (1981) - Preparation of thin targets of ^{239}Pu, ^{233}U and ^{235}U by the method of electrospraying. AAEC/E512.

6.3 Internal Reports

Pearton, S.J. and Lee P.J. (1980) - Electrical properties of polycrystalline GaAs. AP TN 152.

Pearton, S.J. and Lee P.J. (1981) - Electrical properties of polycrystalline Ge (1981), AP TN 153.

Pearton, S.J. (1981) - Electrical properties of γ-irradiated polycrystalline Ge and GaAs, AP TN 156.

6.4 Pamphlets and Books

Ambrose, W.R., Bird, R.J. and Duerden, P. (1981) - The impermanence of obsidian sources in Melanesia. BAR Int. Series 104:1.

Bird, J.R., Duerden, P., Ambrose, W.R. and Leach, B.F. (1981) - Pacific obsidian catalogue. BAR int. Series 104:31.

6.5 Conference Papers

Ambrose, W.R. Duerden, P., Bird, J.R. (1981) - An archaeological application of PIXE-PIGME analysis to Admiralty Islands obsidians. 5th Int. Conf. Ion Beam Analysis, Sydney.

Bird, J.R., Duerden, P., Clapp, R.A. (1981) - Glancing angle measurements of oxygen depth profiles. 5th Int. Conf. Ion Beam Analysis, Sydney.

Bird, J.R., Rose, A. and Wilkins, R.W.T. (1981) - Decoration of dislocations by proton irradiation of halite. 5th Int. Conf. Ion Beam Analysis, Sydney.

Clayton, E., Cohen, D.D. and Duerden, P. - SOXS a computer code for the analysis of X-ray spectra. 5th Int. Conf. Ion Beam Anal., Sydney.

Cohen, D.D. (1981) - M-shell X-ray emission for determining the low energy efficiency of Si(Li) detectors. 5th Int. Symp. X- and γ-ray Source Applications. Ann Arbor, Michigan.

Howard, C.J., Ball, C.J., Elcombe, M.M., Davis, R.L. and Sabine, T.M. (1980) - The AAEC high resolution neutron diffractometer. 12th Meeting of Crystallographers in Australia, Canberra. Poster No. 138.

Lowenthal, G.C. and Page, V. (1981) - Measurements of the areas of gamma peaks with Ge-Li detectors and pulse height analysis operated at 1.0 to 1.5 keV per channel. Scientific Meeting of Int. Comm. for Radionuclide Metrology, Warsaw.

Mouldsworth, J., Lavin, M., Cohen, D.D. (1981) - The sensitivity of ataxia telangiectasia cells to neutrons. 8th AINSE Rad. Biol. Conf., Sydney.

Williams, J.S., Beanland, D.G., Chivers, D.J., Kenny, M.J., Rose, A. and Scott, M. (1981) - Pulsed laser annealing effects in high dose rate silicon implants. Proc. Symp. Laser and Electron Beam-Solid Interactions and Materials Processing; North-Holland, N.Y., pp. 169-175.

Wyllie, H.A. and Lowenthal, G.C. (1981) - Ultra-thin radioactive sources. Scientific Meeting of Int. Comm. for Radionuclide Metrology, Warsaw.

Yehia, H. Abou, Boldeman, J., Fréhaut, J. and Trochon, J. (1981) - Dynamical effects in the neutron induced fission of ^{232}Th. 4th Nat. AIP Physics Congress, Melbourne, Aug. 25-29.

Yehia, H. Abou, Boldeman, J., Pranal, Y. and Trochon, J. (1980) - Comparison of fission characteristics for spontaneous fission and thermal neutron induced fission of some plutonium isotopes. 4th Nat. AIP Physics Congress, Melbourne, Aug. 25-29.

TABLE 1

ACCELERATOR TIME ALLOCATION - 1 OCTOBER 1980 TO 30 JUNE 1981

Category	Experiment Title	Personnel	Origin	Running Time (hours)
Applications	Oxides	Bird, Duerden, Cohen, Smith, Clapp	Appl. Phys/AINSE/NSWIT	124
	Glass	Bird, Rose	Appl. Phys.	18
	Biological samples	Clayton, Wooler	Appl. Phys/NSW Health Comm.	179
	Halite	Bird	Appl. Phys.	40
	Tungsten thickness	Gillespie, Cohen	Materials/AINSE	9
	Obsidian	Duerden, Ambrose, Specht, Leach	Appl. Phys/ANU/Aust. Museum/ Otago	65
	Clay	Duerden, Rye, Allen, Longmore	Appl. Phys/ANU/Griffith	91
Nuclear Physics	Fission	Boldeman, Walsh	Appl. Phys.	207
	Capture	Boldeman	Appl. Phys.	17
Ion Implantation	RBS	Kenny, Rose, Scott	Appl. Phys.	193
	RBS	Williams	RMIT	155
	RBS	Wagh	Trombay	17
Semiconductor and Radiation Physics	Semiconductor surface studies	Lawson	Appl. Phys.	86

TABLE 1 (cont'd)

Category	Experiment Title	Personnel	Origin	Running Time (hours)
AINSE Projects	Neutron irradiation of cells	Lavin	Queensland	70
	F in coal	Tiller	Darling Downs	68
	Hydrogen profiling	Livick, Harding	Sydney	7
	Si wafers	Golja, Nassibian	University of Western Australia	19
	Miscellaneous	Cohen	AINSE	51
Accelerator tests				70

Total running time	1486
Maintenance and development	554
Unused time	6720

TABLE 2

MEASURED AND LITERATURE CONCENTRATIONS

($\mu g\ g^{-1}$ or % weight) FOR THE USGS STANDARDS

BCR1 AND W1

The bracketed values are for information only

Element	BCR1			W1		
	Measured	Literature	% Difference	Measured	Literature	% Difference
Ca %	3.82	4.9	22	6.7	7.8	14
Cl	218			155	(200)	23
Cr		(17.6)		106	114	7
Cu	15	18.4	18.4	126	110	15
Fe %	8.54	9.37	8.8	7.4	7.8	5
Ga	21	(20)	5	18.4	16	14
K %	1.1	1.4	21	0.4	0.5	20
Mn	1412	1406	0.4	1108	1280	8
Ni		(15.8)		54	76	28
P	1566	1570	0.25			
Rb	56	46.6	20	39	21	85
Si %	24.4	25.4	3.9	24.4	24.6	0.8
Sr	332	330	0.6	192	190	1
Ti %	1.0	1.28	21	0.60	0.64	6
V	271	(339)	32	238	264	10
Y	46	(37.1)	24			
Zn	116	120	3.3	88	86	2
Zr	182	(190)	4.2	52	105	50

TABLE 3

PERFORMANCE OF DUOPLASMATRON ION SOURCE
BEAM ENERGY = 20 keV

Gas	Beam Current (μA)	
	10mm diameter	20mm diameter
Hydrogen	60	360
Nitrogen	50	330
Argon	25	225

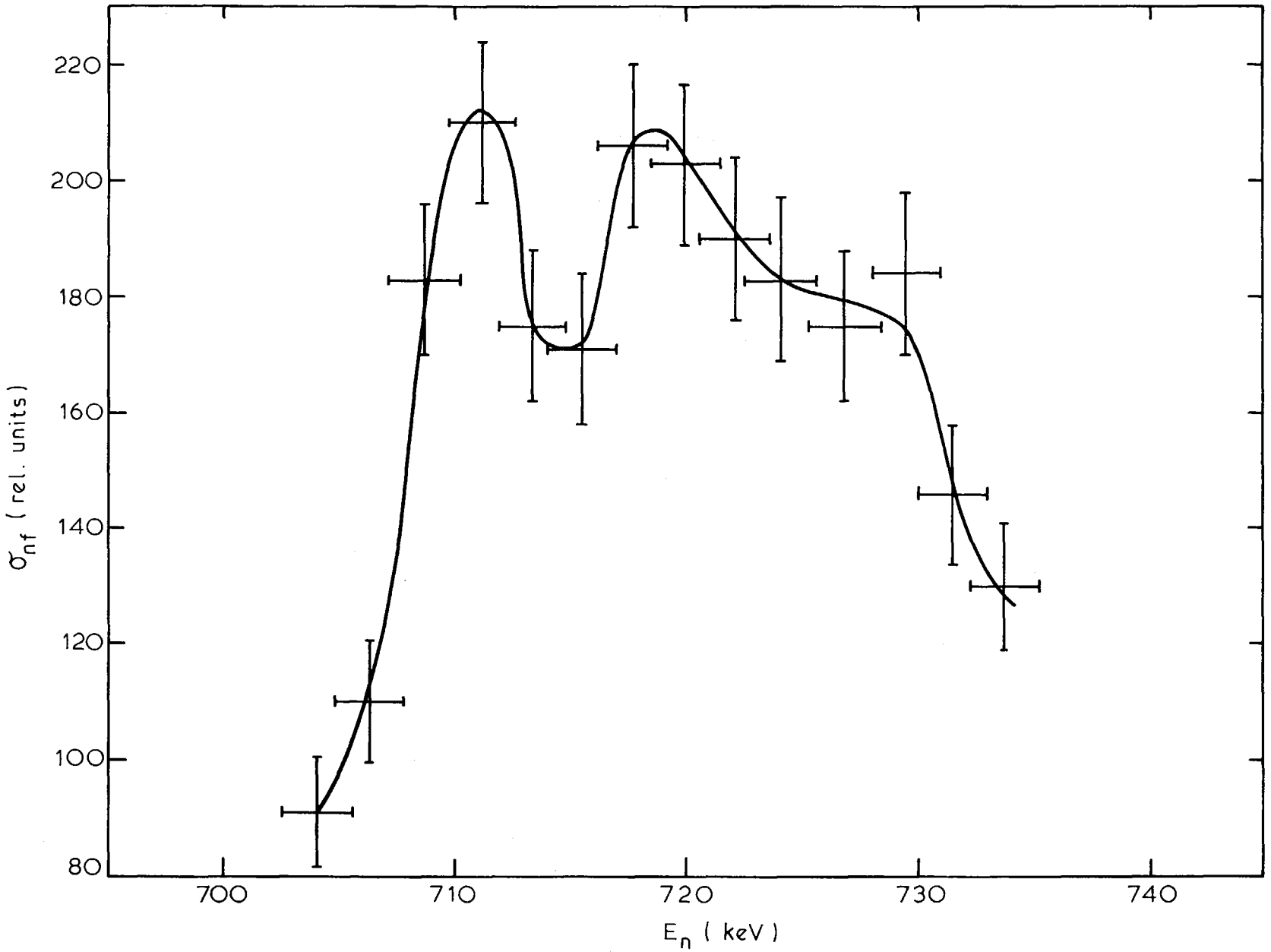

Figure 1 NEUTRON FISSION CROSS SECTION σ_{nf} FOR ^{230}Th

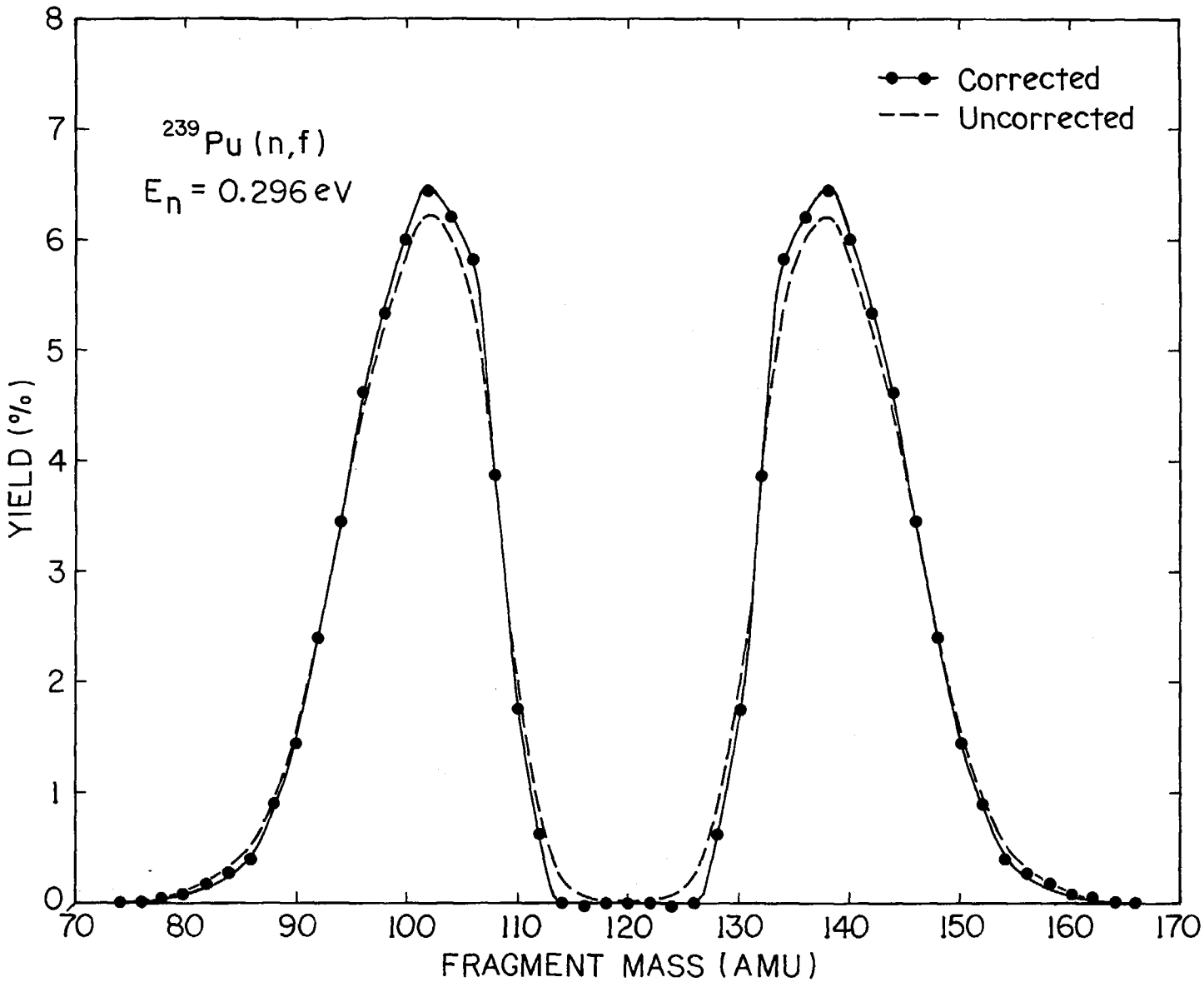

Figure 2 Pre-neutron emission mass distribution for ^{239}Pu(n,f) for E_n=0.296 eV, corrected for mass resolution by polynomial inversion operator method.

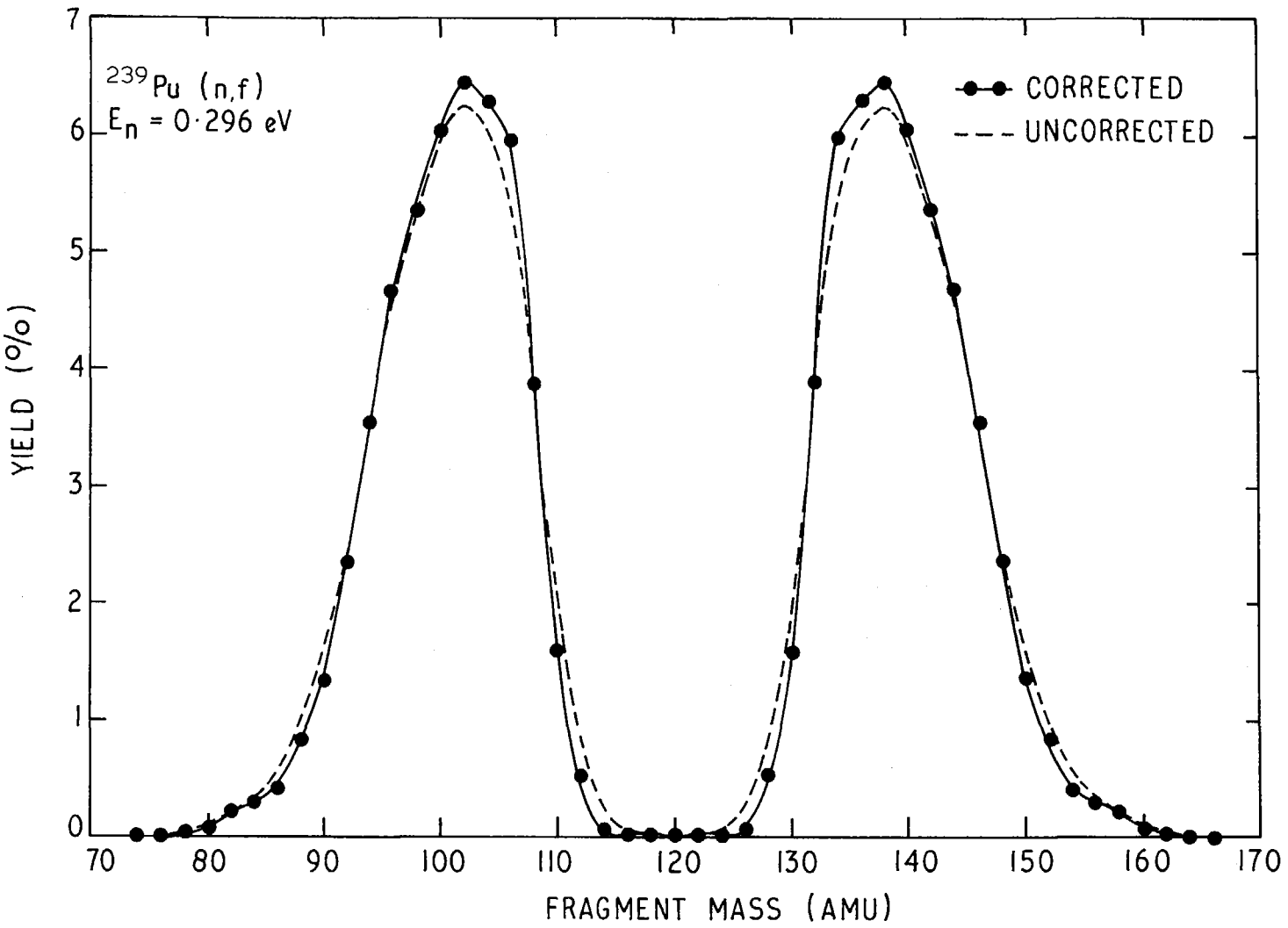

Figure 3 Pre-neutron emission mass distribution for ^{239}Pu(n,f) for E_n=0.296 eV, corrected for mass resolution by conjugate gradient iterative method.

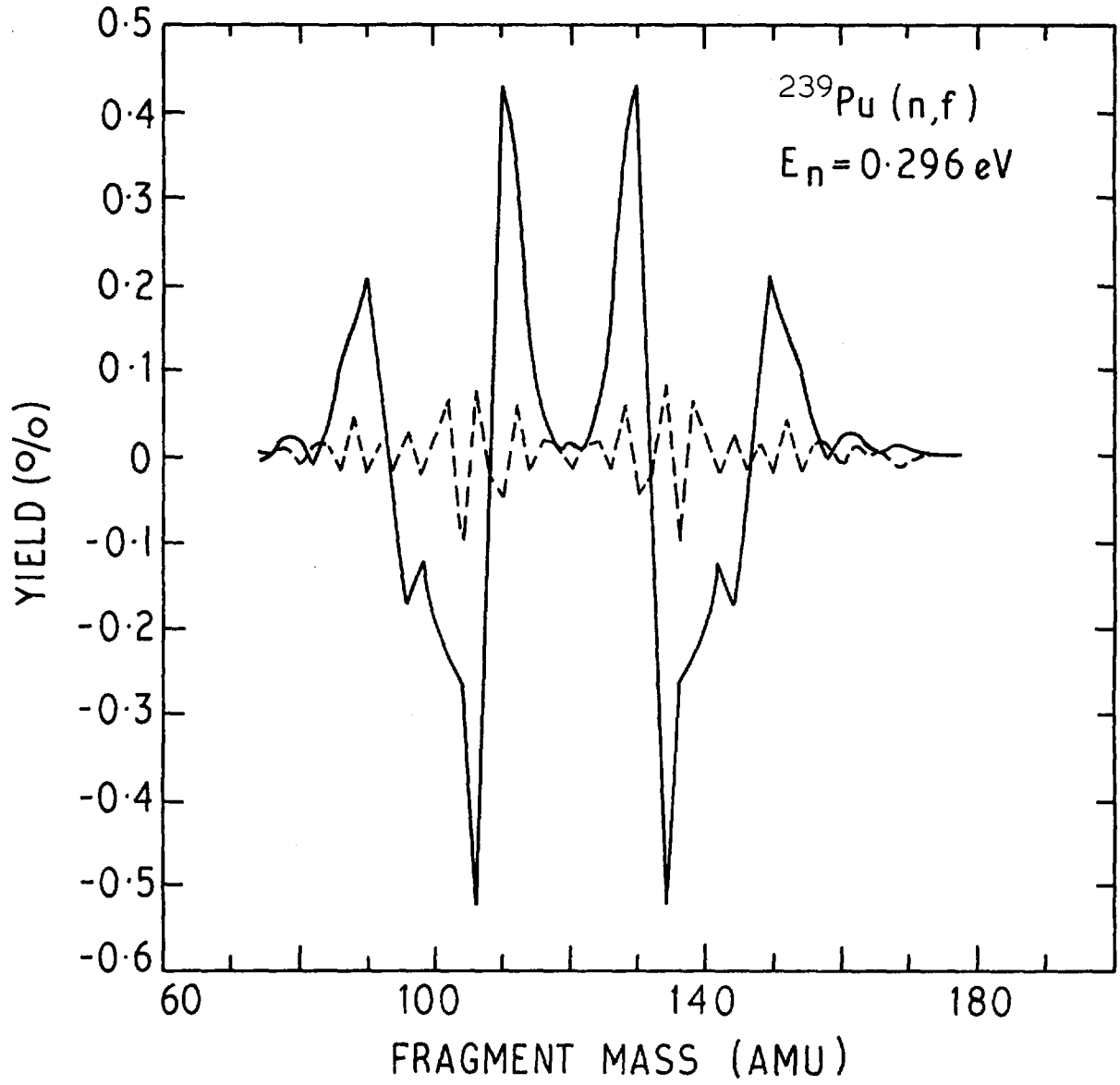

Figure 4 The effects of iterative conjugate gradient unfolding, after five iterations. The difference between the unfolded mass spectrum and the raw data is shown (solid line). The fit to the data is illustrated on the same scale with a plot of the residual discrepancies obtained by subtracting the reconstructed data from the measured data (dashed line).

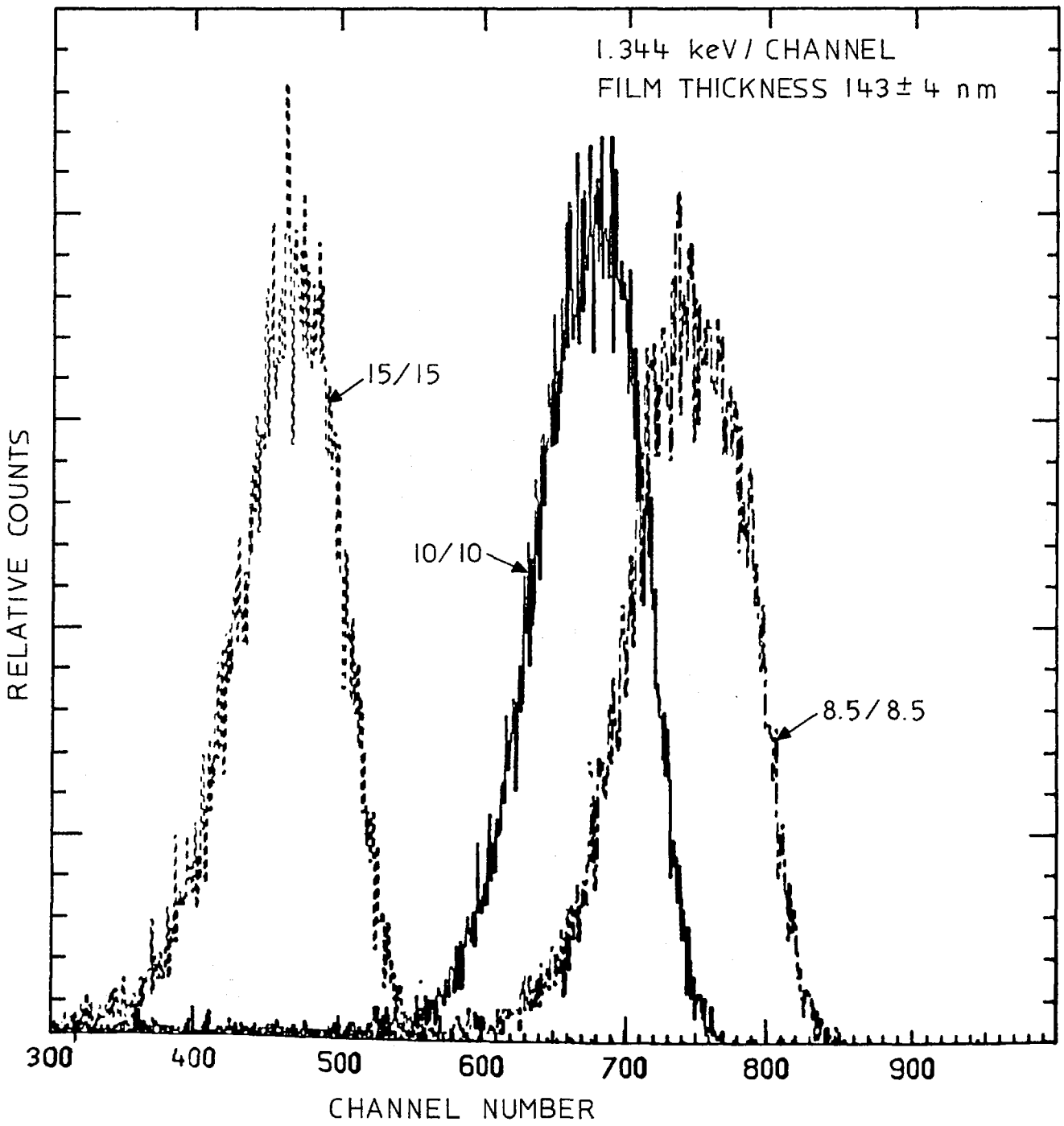

Figure 5 Proton spectra from a 143± 4nm hydrogen film on a copper substrate with various incident α-particle and emergent proton glancing angles to the surface.

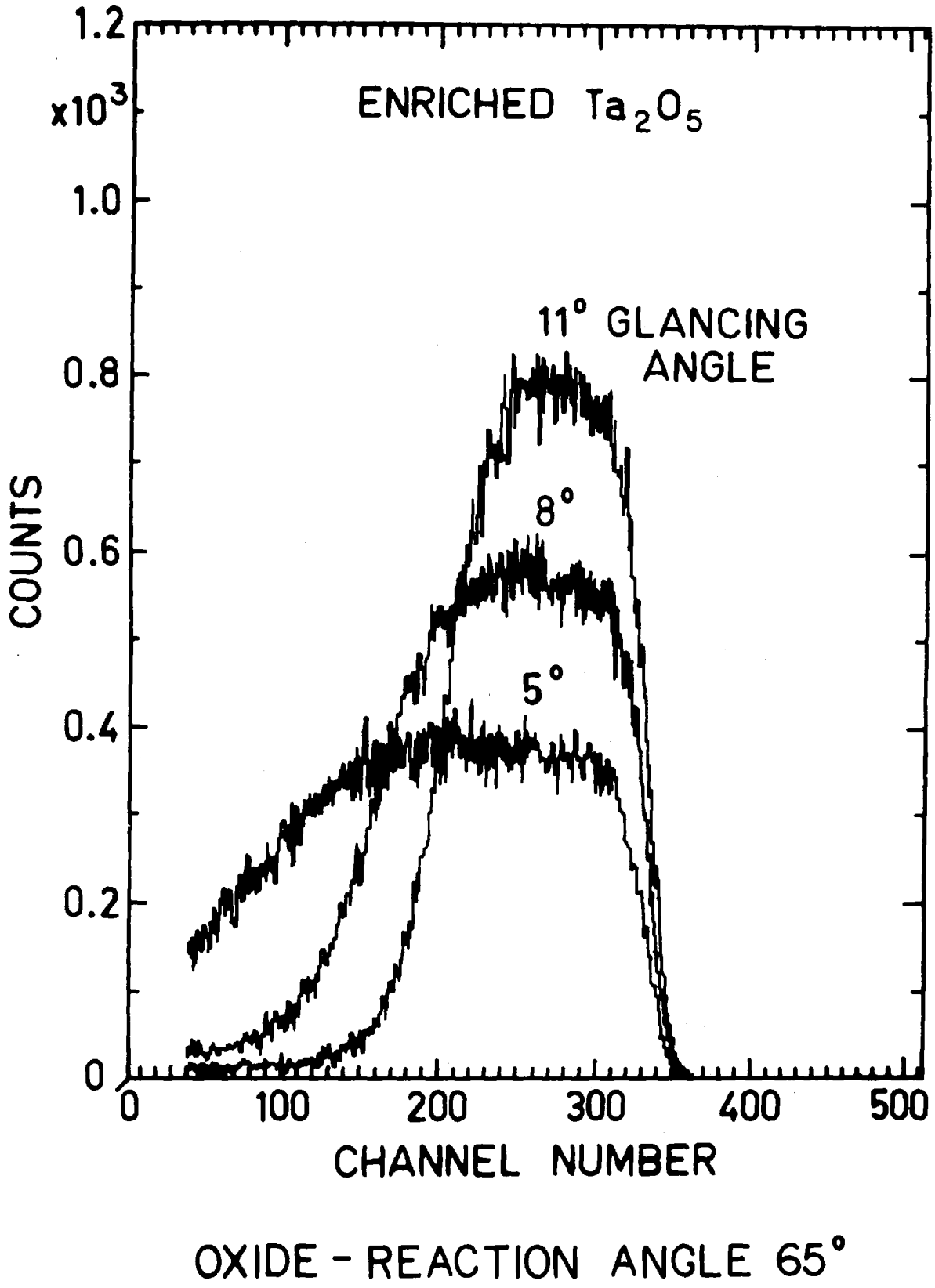

Figure 6 $^{18}O(p,\alpha)$ energy spectra from a 500 nm oxide layer (12% ^{18}O) for a reaction angle of 65° and glancing angles of 5, 8 and 11°.

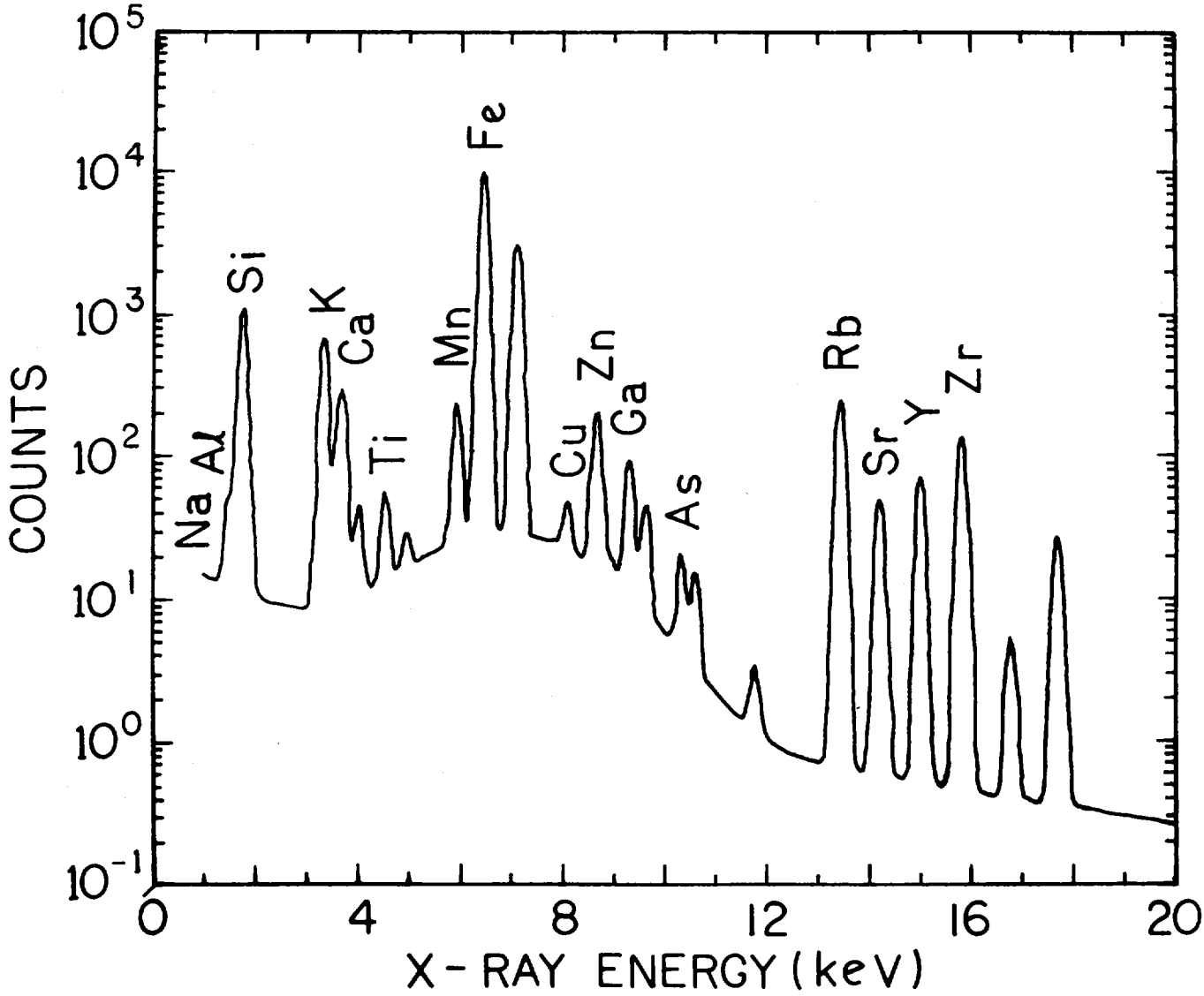

Figure 7 Synthesis of an X-ray spectra without filters of a typical obsidian sample. The spectrum is dominated by counts from the light elements.

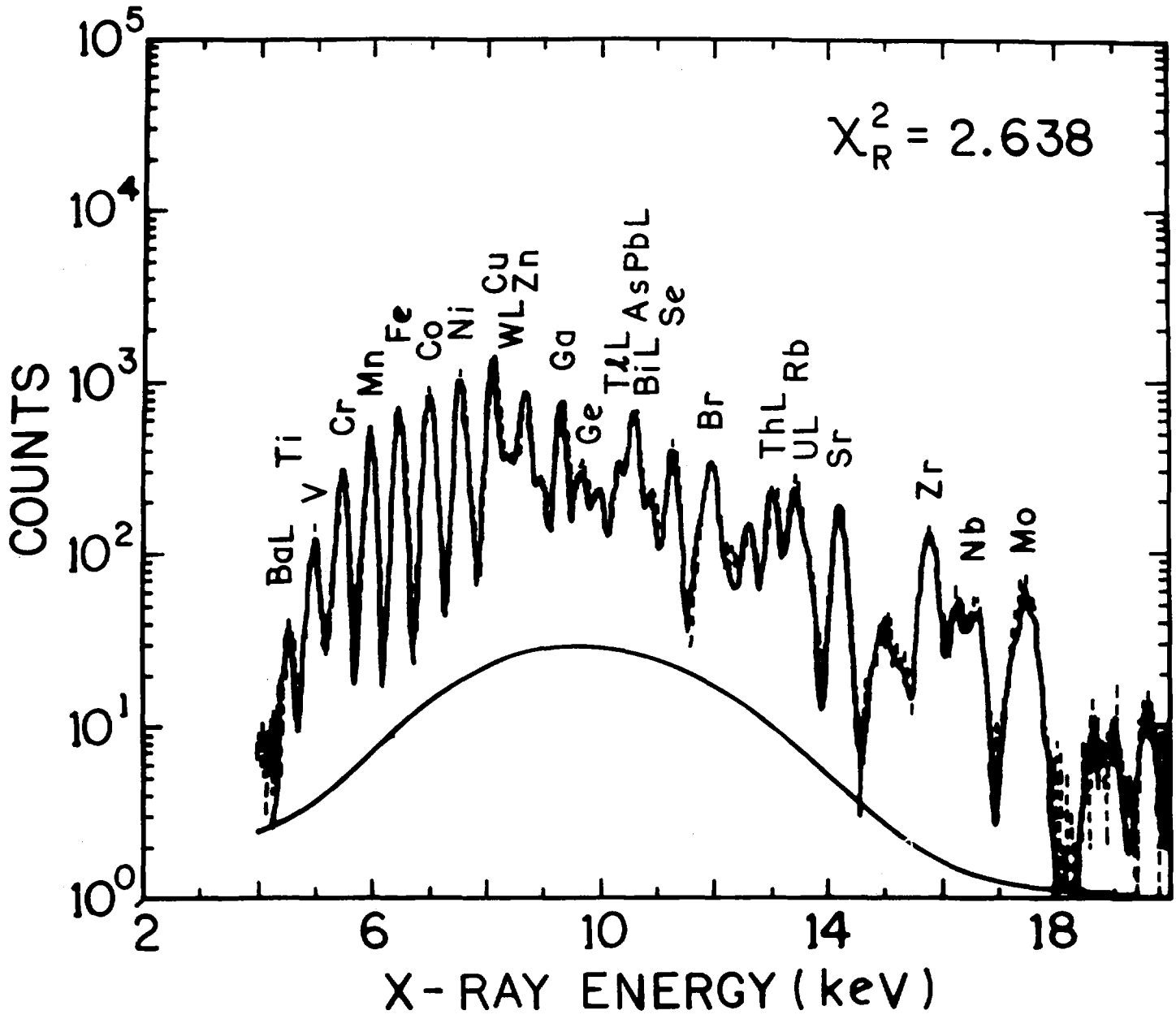

Figure 8 The X-ray spectrum between 4 and 20 KeV for the multi-element standard in graphite. Twenty-six elements are detected in this range.

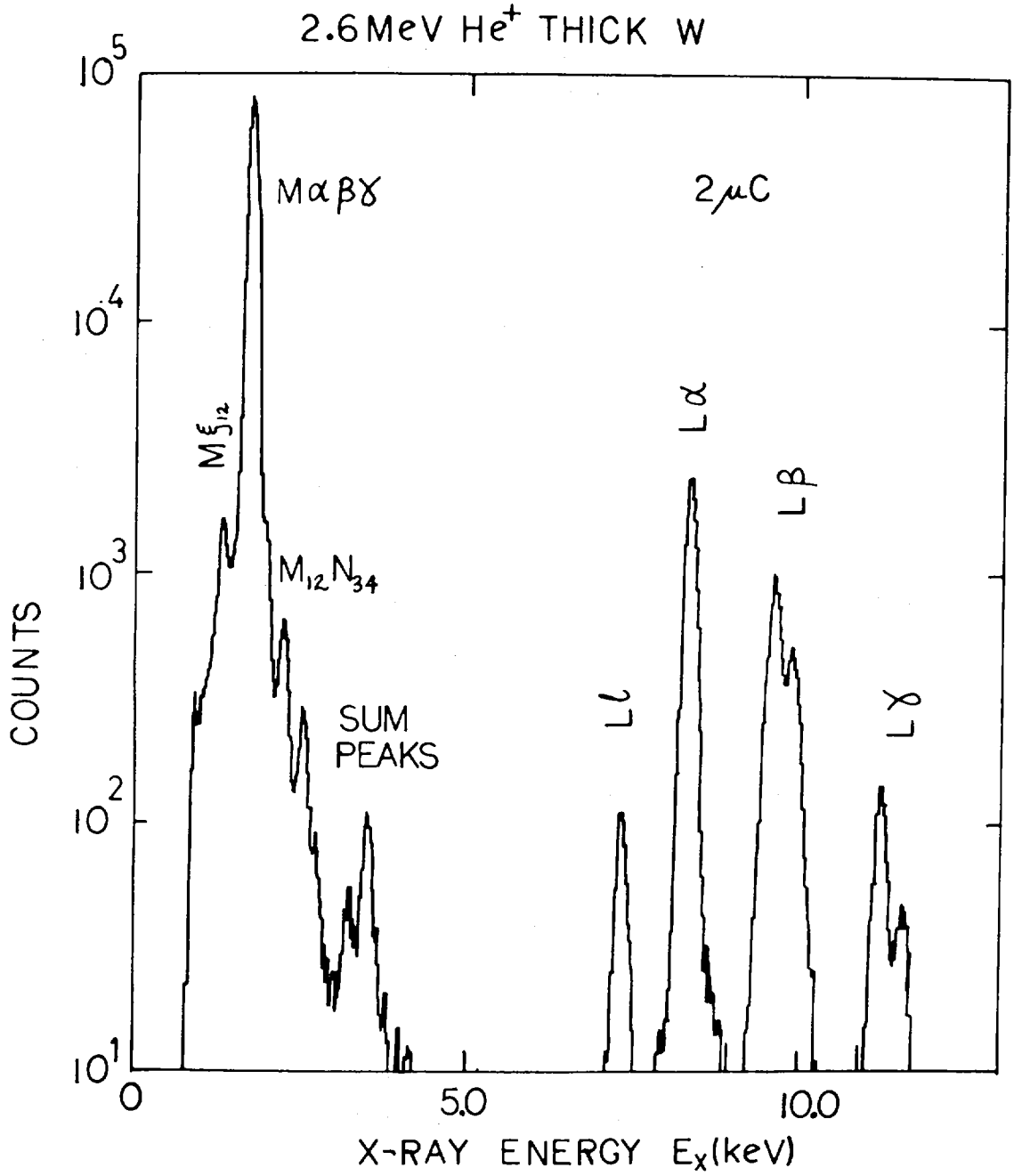

Figure 9 Typical X-ray spectrum for 2.6 MeV He^+ bombardment of thick W, 2 μC total charge and a solid angle $\Omega = 3.1 \times 10^{-4}$ sr.

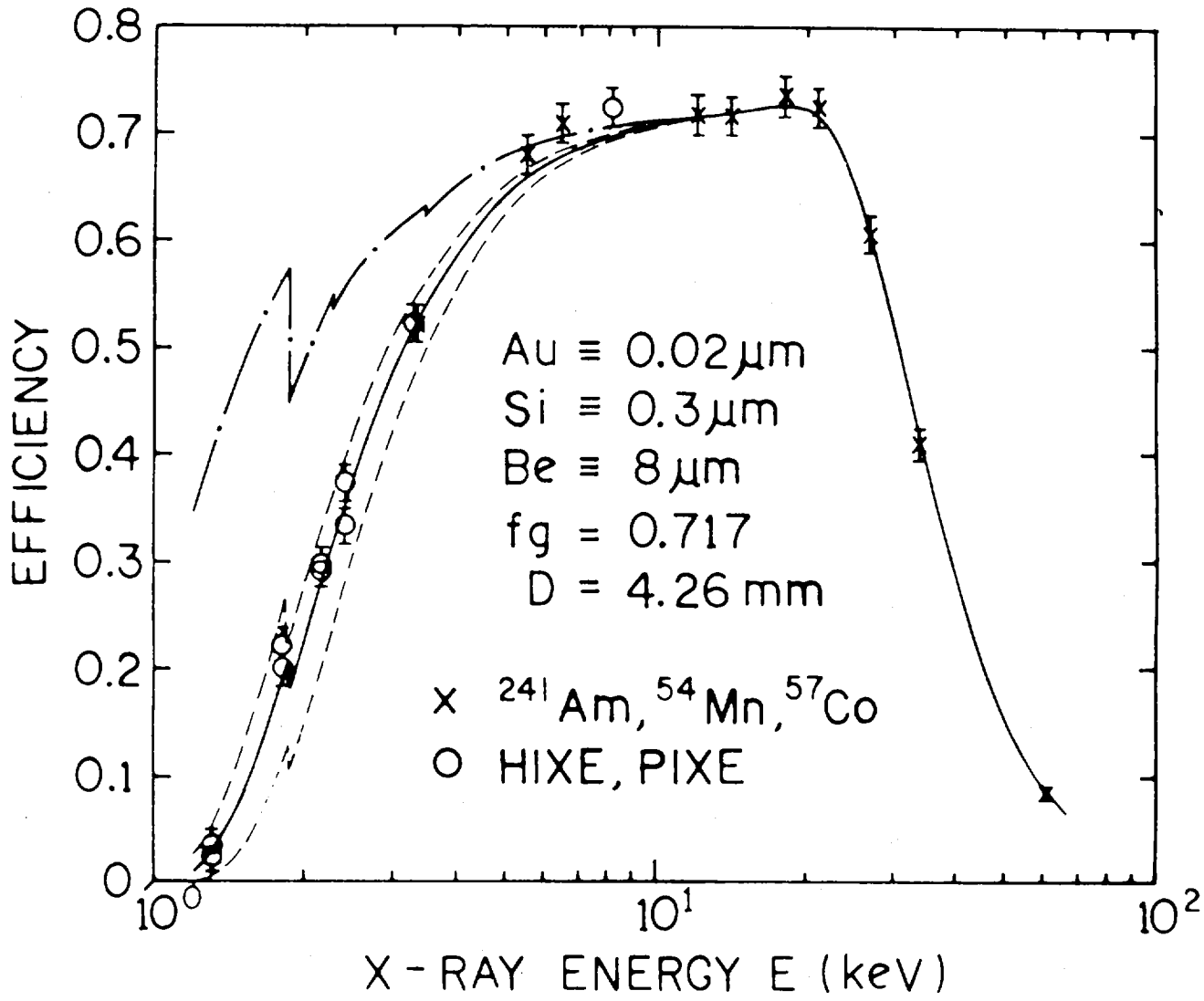

Figure 10 Si(Li) detector efficiency versus X-ray energy. f_{Be} ≡ 8 μm, f_{Si} ≡ 0.3 μm, f_{Au} ≡ 0.02 μm and f_g = 0.717. f_{Be}, f_{Si} and f_{Au} are correction factors representing the quated thicknesses of Be, Si and Au. f_g is the geometric factor[24]. Detector thickness D ≡ 4.26 mm. The points (o,x) are the experimentally measured points. The (x) are for source determinations and are taken from reference[24]. The (o) are the present HIXE and PIXE work. The chained curve is for f_g = 1.00 and represents zero ice build-up on the detector; the solid curve is the lease squares fitted curve to the data and represents an ice thickness of 13 μm. The dashed curves are the 3σ standard deviation of the results about the solid curve and represents an ice thickness variation of 10 to 18 μm of ice.

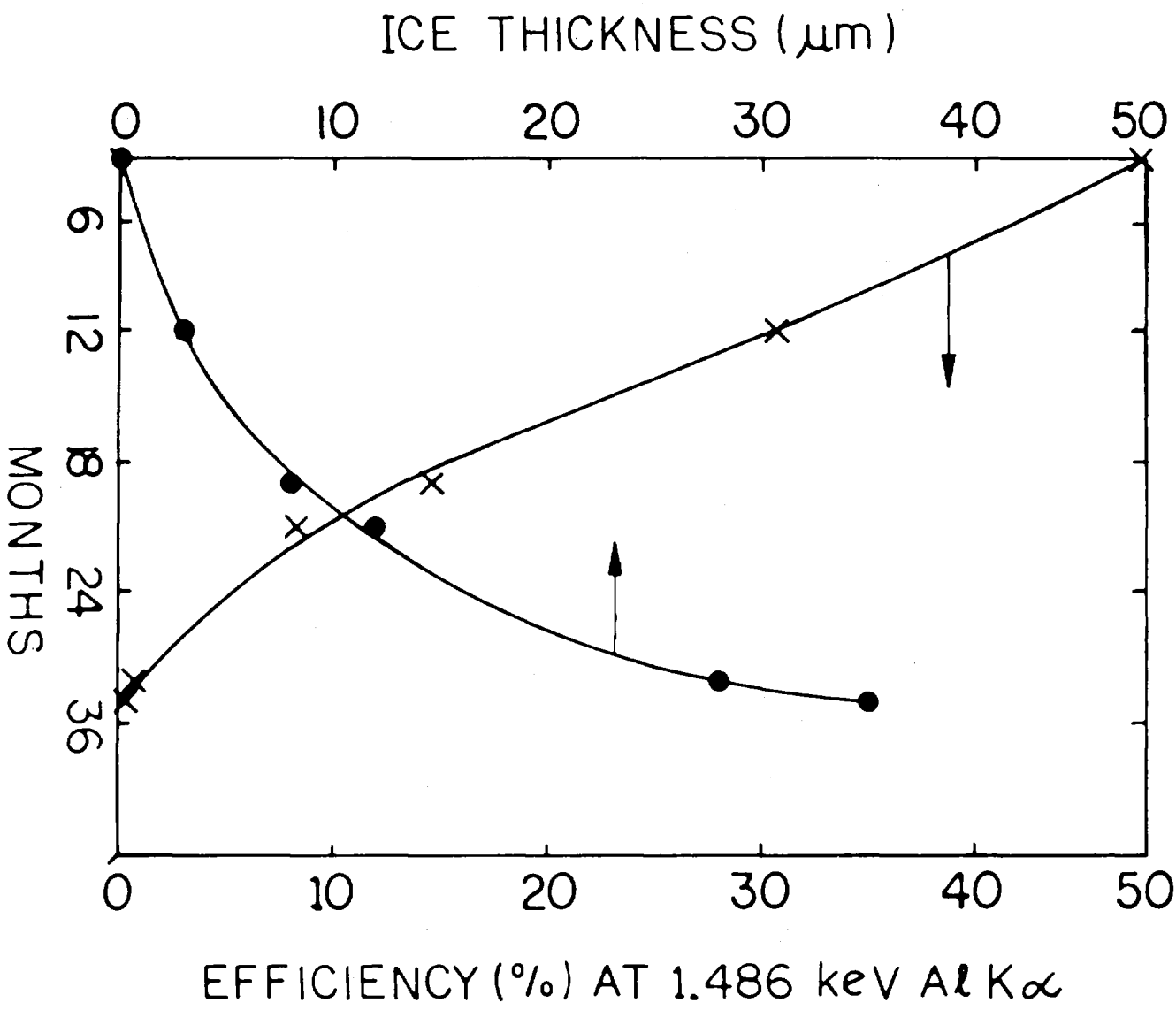

Figure 11 Ice build-up versus time (full circles). The equivalent detector efficiency (crosses) for Al Kα X-rays at 1.486 keV is also shown as a function of time.

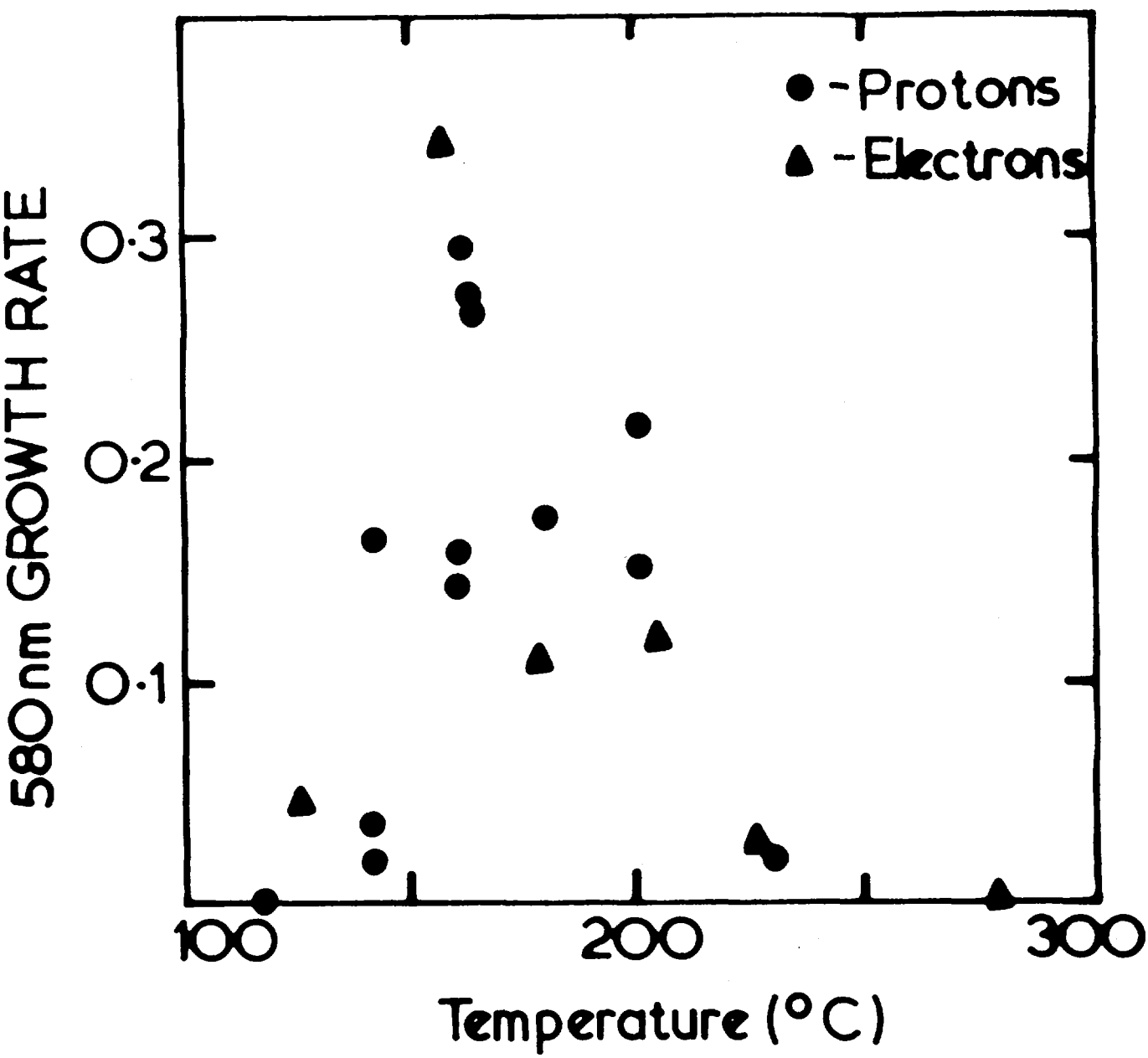

Figure 12 Dependence of the linear growth rate of 580 nm absorption on sample temperature. Circles are for the present proton experiment; triangles for the electron experiment of Swyler et al. 26a).

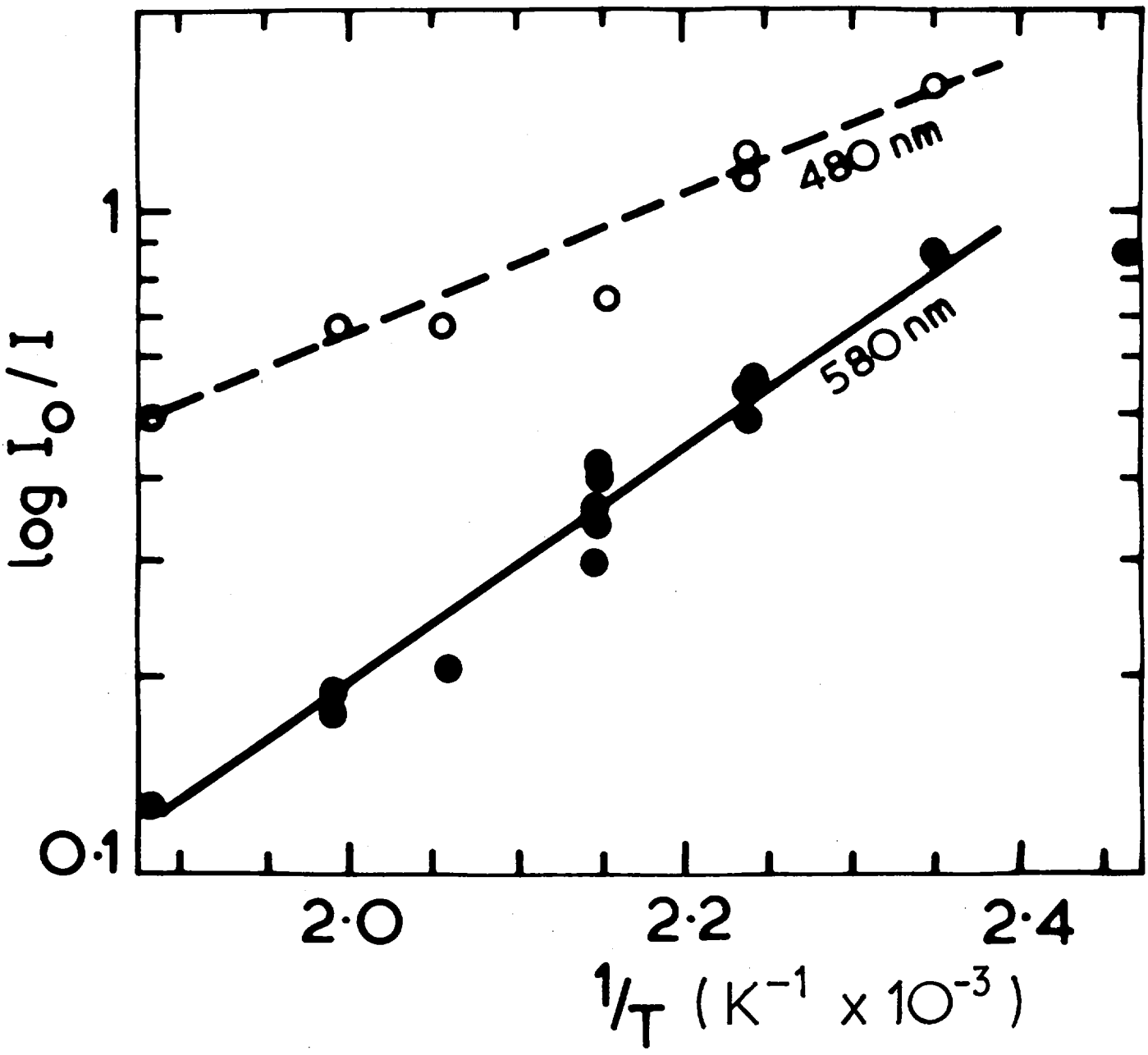

Figure 13 Dependence of 480 nm (open circles) and 580 nm (solid circles) saturation absorption on sample temperature.

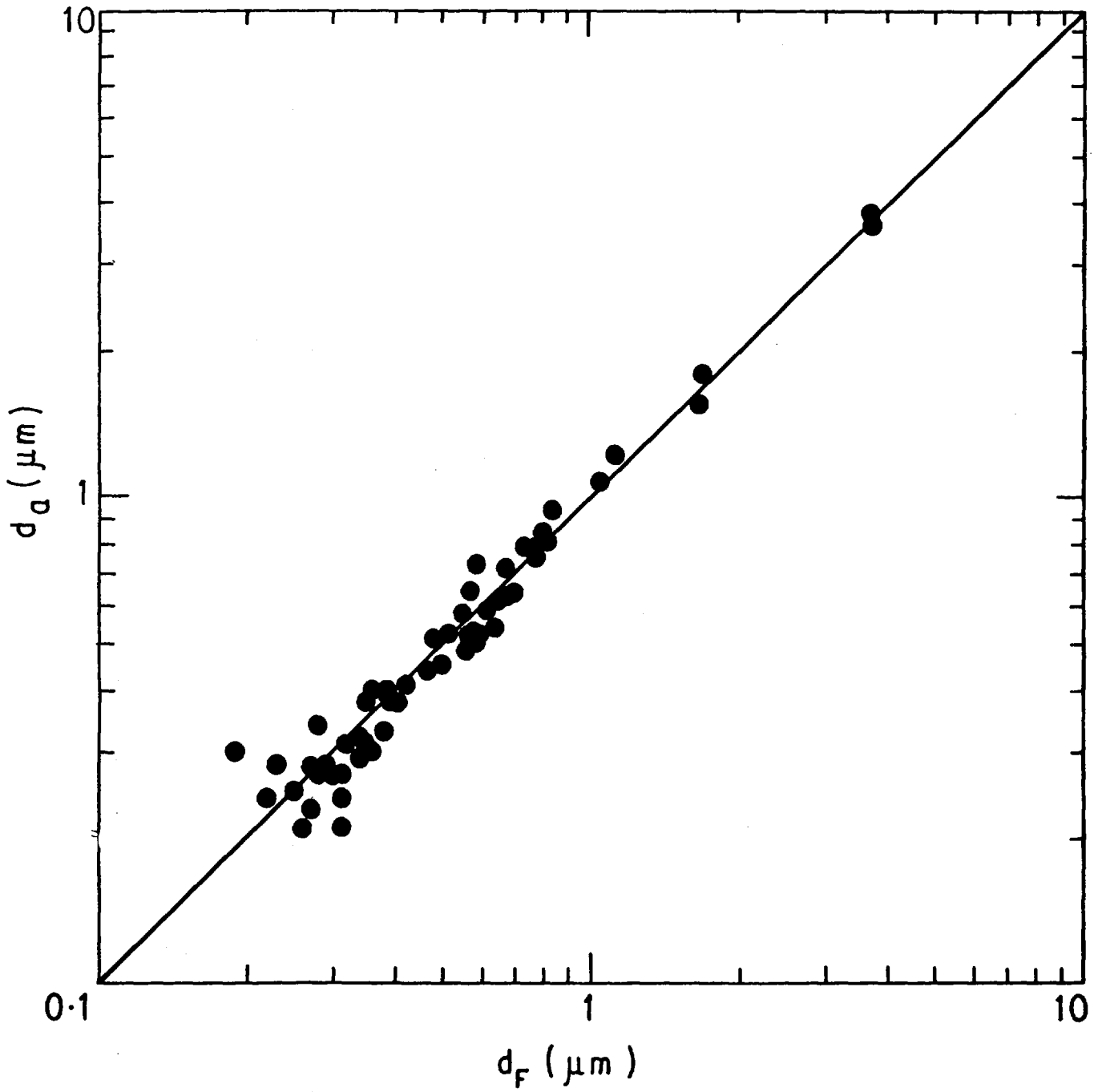

Fig. 14. PuO_2 particle diameters. d_F = particle diameter from fission track detector. d_a = particle diameter from alpha detector.

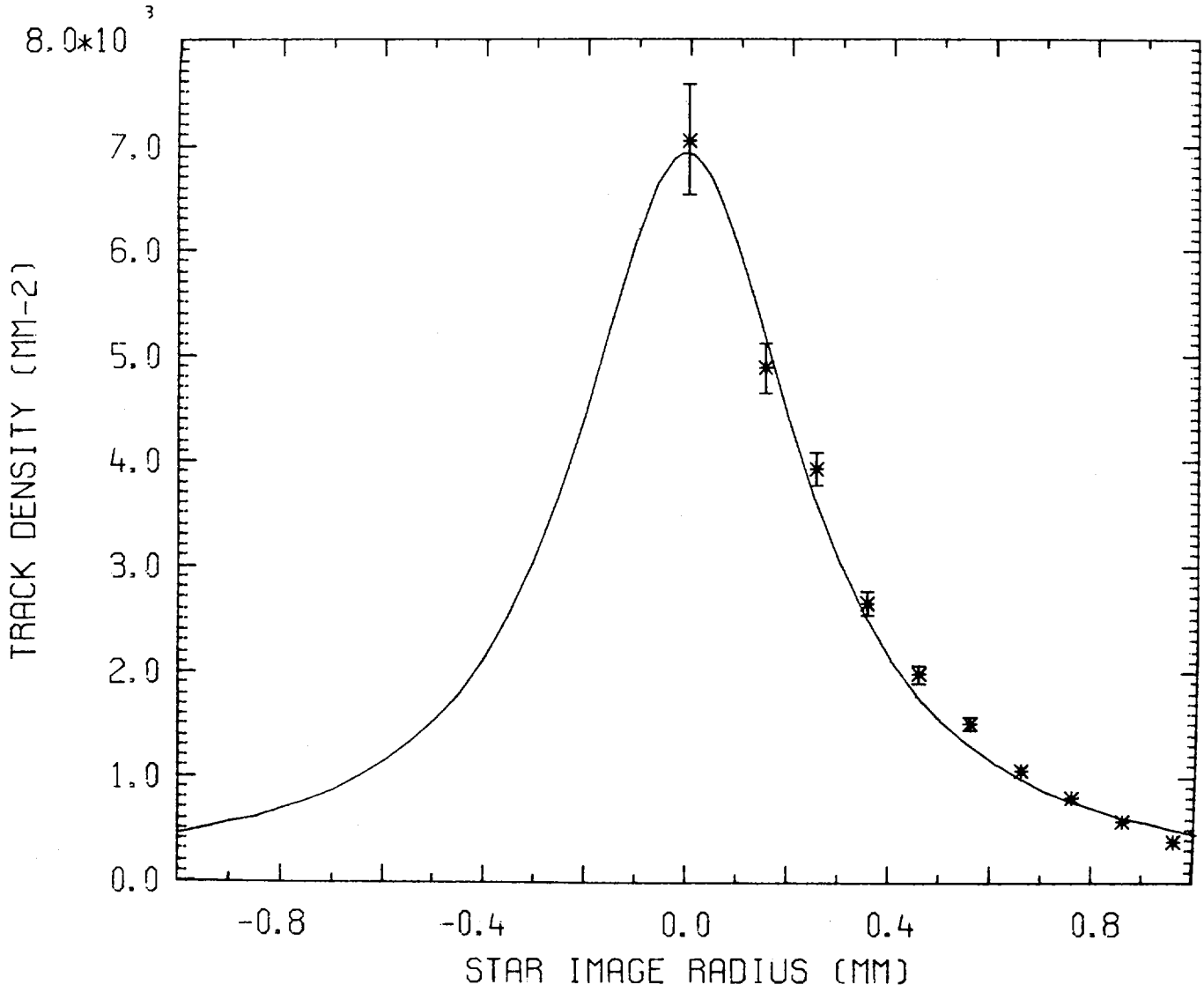

Figure 15 Alpha particle track density distribution from a point source of PuO_2.

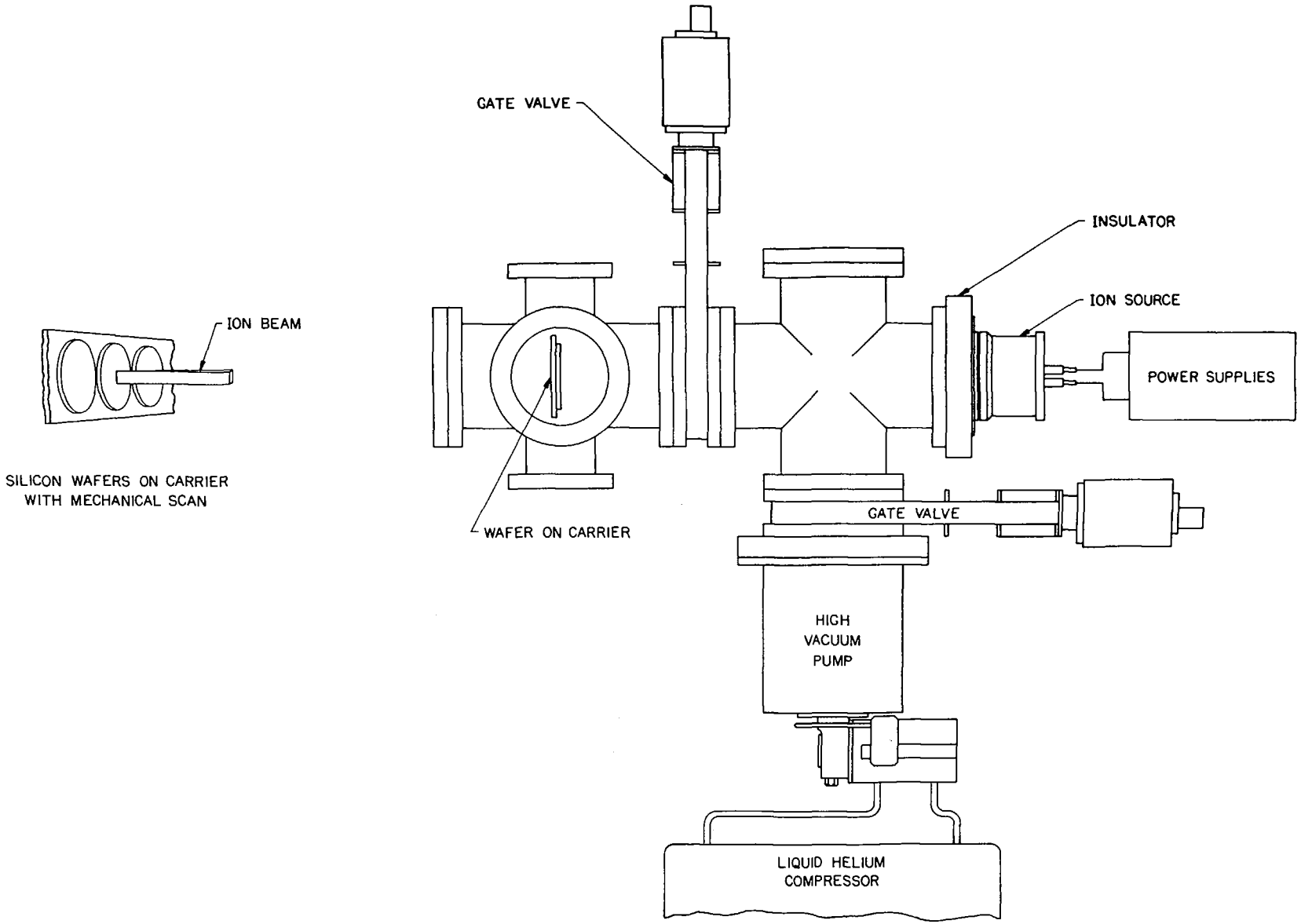

Figure 16 Experimental layout of Ion Implanter with no mass analysis of ion beam.

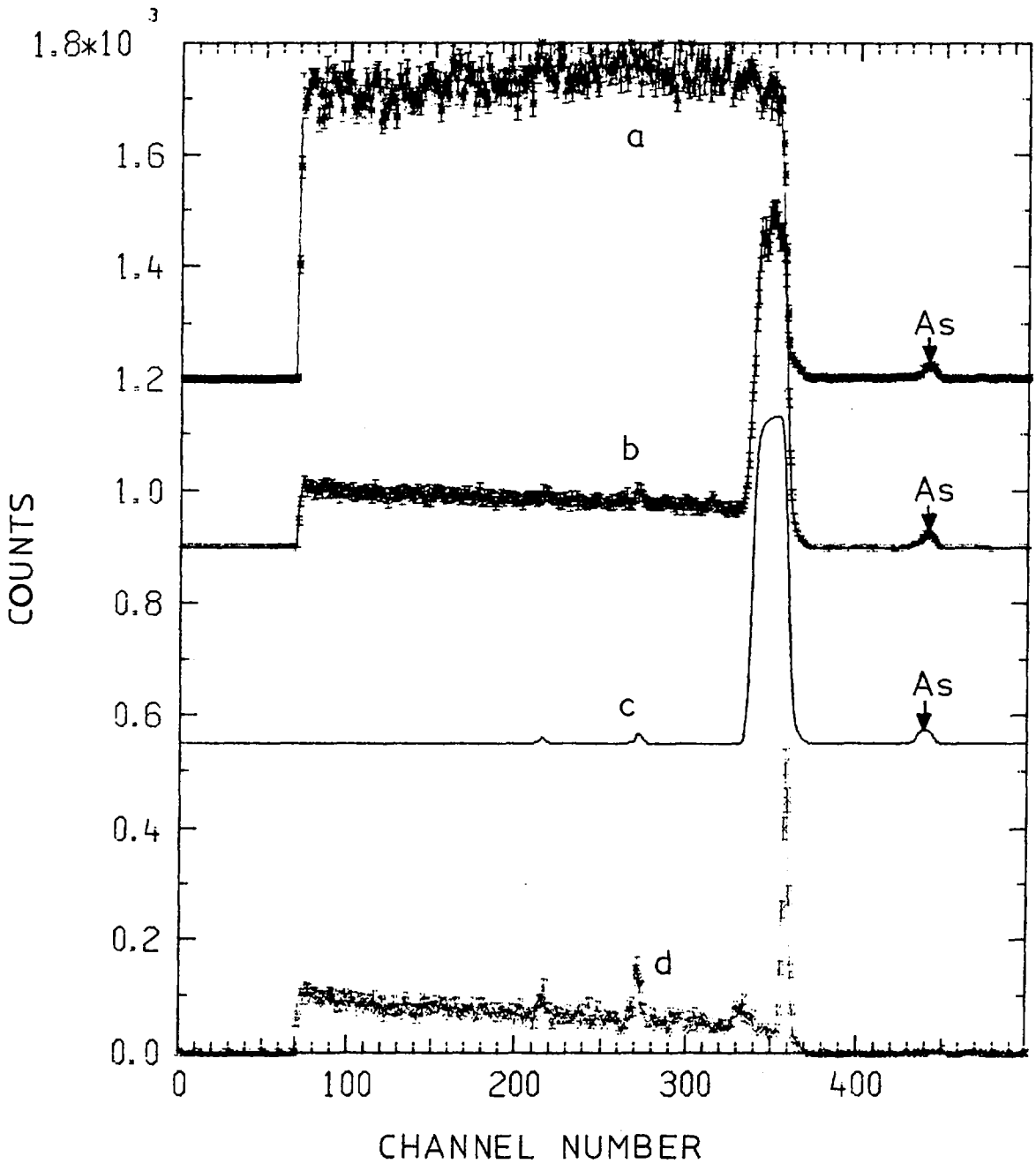

Figure 17 Backscattering spectra for arsenic implanted in silicon.

(a) Random. (b) Aligned along <110> axis.
(c) Calculated spectrum for (b).
(d) Aligned and annealed.

DISTRIBUTION LIST - AAEC/AP PR81

1. Chairman
2. Deputy Chairman
3. Professor M. Brennan
4. Sir Bernard Callinan
5. Director
6. Deputy Director, Operations
7. Deputy Director, Research
8. Chief Scientist, Nuclear Fuel Cycle
9. Chief, Applied Mathematics and Computing Division
10. Chief, Centrifuge Enrichment Project Division
11. Chief, Environmental Science Division
12. Chief, Isotope Division
13. Chief, Materials Division
14. Chief, Nuclear Technology Division
15. Chief, Applied Physics Division
16. Head, Technical Secretariat
17. Secretary
18. Director, Public Relations
19. Director, Regulatory Bureau
20. Controller, Site Information Services
21. Executive Officer, AINSE
22-24. Library
25. Vienna Office
26-66. J.W. Boldeman (for INDC and Bilateral Agreement correspondents)
67-96. J.R. Bird (for special distribution)
97. B.J. Allen
98. W.K. Bertram
99. J.W. Boldeman
100. G.M. Carter
101. B.E. Clancy
102. E. Clayton
103. J.W. Connolly
104. J.L. Cook
105. D.D. Cohen
106. M. Dilli
107. P. Duerden
108. G. Durance
109. I.J. Donnelly
110. A.W. Dalton
111. J.E. Eberhardt
112. P.J. Ellis
113. C.P. Gilbert
114. R.M. Hicks
115. G.R. Hogg
116. M.J. Kenny
117. D.W. Lang
118. E.M. Lawson
119. G.C. Lowenthal
120. D.B. McCulloch
121. B.J. McGregor
122. P.C. Miskelly

DISTRIBUTION LIST (continued)

123. A.R.D. Musgrove
124. A.W. Pryor
125. M.T. Rainbow
126. D.J. Reid
127. G.S. Robinson
128. E.K. Rose
129. A. Rose
130. M.D. Scott
131. A.J. Tavendale
132. J. Tendys
133. W.J. Turner
134. D.F. Urquhart
135. G.C. Wall
136. T. Wall
137. R.L. Walsh
138. G.C. Watt
139. D.J. Wilson
140. H.A. Wyllie
141. D. Byers (University of Canterbury, N.Z.)
142. S. Supadi (BATAN, Bandung)
143. I. Supki (BATAN, Bandung)
144. G. Tyror (AEEW, U.K.)
145. J. Askew (AEEW, U.K.)
146-166. Bilateral Agreements (UKAEA 5, US Dept. of Energy 11, AECL 5)
167-196. Spares